JOURNAL OF NEUROTRAUMA 32:875–892 (June 15, 2015)
DOI: 10.1089/neu.2013.3321

A Consistent, Quantifiable, and Graded Rat Lumbosacral Spinal Cord Injury Model

Junxiang Wen,[1,2] Dongming Sun,[1] Jun Tan,[2] and Wise Young[1]

Abstract

The purpose of this study is to develop a rat lumbosacral spinal cord injury (SCI) model that causes consistent motoneuronal loss and behavior deficits. Most SCI models focus on the thoracic or cervical spinal cord. Lumbosacral SCI accounts for about one third of human SCI but no standardized lumbosacral model is available for evaluating therapies. Twenty-six adult female Sprague-Dawley rats were randomized to three groups: sham ($n=9$), 25 mm ($n=8$), and 50 mm ($n=9$). Sham rats had laminectomy only, while 25 mm and 50 mm rats were injured by dropping a 10 g rod from a height of 25 mm or 50 mm, respectively, onto the L4-5 spinal cord at the T13/L1 vertebral junction. We measured footprint length (FL), toe spreading (TS), intermediate toe spreading (ITS), and sciatic function index (SFI) from walking footprints, and static toe spreading (STS), static intermediate toe spreading (SITS), and static sciatic index (SSI) from standing footprints. At six weeks, we assessed neuronal and white matter loss, quantified axons, diameter, and myelin thickness in the peroneal and tibial nerves, and measured cross-sectional areas of tibialis anterior and gastrocnemius muscle fibers. The result shows that peroneal and tibial motoneurons were respectively distributed in 4.71 mm and 5.01 mm columns in the spinal cord. Dropping a 10-g weight from 25 mm or 50 mm caused 1.5 mm or 3.75 mm gaps in peroneal and tibial motoneuronal columns, respectively, and increased spinal cord white matter loss. Fifty millimeter contusions significantly increased FL and reduced TS, ITS, STS, SITS, SFI, and SSI more than 25 mm contusions, and resulted in smaller axon and myelinated axon diameters in tibial and peroneal nerves and greater atrophy of gastrocnemius and anterior tibialis muscles, than 25 mm contusions. This model of lumbosacral SCI produces consistent and graded loss of white matter, motoneuronal loss, peripheral nerve axonal changes, and anterior tibialis and gastrocnemius muscles atrophy in rats.

Key words: immunohistochemistry; locomotor function; models of injury; rat; spinal cord injury

Introduction

The lumbosacral spinal cord includes the lumbar enlargement and sacral segments of the spinal cord, containing most of the neurons that innervate the legs and pelvic organs. Located in the T11 to L1 vertebral segments, the lumbosacral spinal cord ends just below the L1 vertebra and the cauda equina fills the spinal canal from L1 to S5 vertebra. Spinal cord injury (SCI) at the T12 or L1 vertebral segment not only interrupts long spinal tracts but also damages gray matter containing neurons that innervate legs and pelvic organs, as well as lumbosacral spinal roots that run alongside the spinal cord.

The National SCI Database[1] reports that 55% and 35% of SCI involve the cervical and thoracic spine, respectively, in the United States, suggesting only 10% of SCI are lumbosacral. This likely underestimates lumbosacral SCI since T10-T11 injuries damage lumbosacral cord and as many as 15% of cervical and thoracic SCI have associated lumbosacral injuries.[2] Lack of spasticity after injury may indicate lumbosacral SCI since cervical or upper thoracic injuries are associated with spasticity; however, up to 22% of patients with cervical and thoracic SCI have flaccid paralysis.[3] If these 22% of patients were added to the 10% of L1 vertebral injuries, a third of SCI would involve the lumbosacral cord. Wang and colleagues[4] reported that cervical SCI accounted for 46.3%, thoracic 20.4%, and lumbosacral 33.3% of SCI in Anhui province, China.

The lumbosacral spinal cord contains critical motor centers, including the central pattern generator (CPG) for locomotion, Onuf's nucleus for micturition, and sacral nuclei that control anal and sexual functions. Damage to these centers disrupts crucial motor programs. Loss of motoneurons causes flaccid paralysis and atrophy of limbs, the bladder, and anal muscles. Lumbar and sacral

[1]Department of Cell Biology and Neuroscience, Rutgers, the State University of New Jersey, Piscataway, New Jersey.
[2]Department of Orthopaedics, Tongji University School of Medicine, Shanghai, China.

spinal roots run alongside the spinal cord at T11- L1. Lumbosacral trauma may damage the spinal roots.[5] Finally, 10 segments (L1-S5) of lumbosacral spinal cord and their roots are squeezed into three vertebral segments (T12-L1). Injury to one vertebra can compromise multiple spinal cord segments.

Most animal SCI models have focused on the cervical[6] or thoracic spinal cord.[7] Injuring methods include transection,[8] hemisection,[9,10] contusion,[11–14] or compression.[15,16] In thoracic SCI models, the major consequence is damage to long spinal tracts and consequent sensory and motor loss.[17,18] Thoracic gray matter includes sensory neurons, interneurons, and motoneurons that innervate multiple segments of axial musculature. Thoracic damage causes functional loss due to long tract damage. Magnuson and colleagues[17] found that injecting the neurotoxin kainic acid (KA) into T9 spinal cord killed gray matter, preserved white matter, and did not contribute to locomotor deficits in rats. In contrast, T9 contusion caused marked loss of locomotor function. KA injections into L2 spinal cord caused only gray matter damage but nevertheless caused severe locomotor deficits. Contusion of L2 spinal cord containing the central pattern generator also causes severe locomotor deficits.

Repairs of thoracic SCI have usually focused on regenerating or remyelinating ascending and descending white matter tracts. Different therapeutic approaches are required for repairing injuries involving gray matter loss.[17] These include replacing interneurons and motoneurons, as well as regenerating long tracts to innervate these neurons and coaxing the motoneurons to grow their axons into the ventral roots to innervate muscle. To test therapeutic strategies for restoring function after gray matter injuries, consistent animal SCI models involving gray matter loss in the cervical or lumbosacral spinal cord are required. Several cervical SCI models are available.[6,19–23] Most cervical SCI models utilize unilateral upper cervical hemisections, hemicontusions, or bilateral lower cervical contusions that cause partial injuries of the spinal cord.[22,24] Such partial injury models usually allow rats to recover substantial hindlimb locomotion due to contralateral sprouting of serotonergic fibers in the lumbosacral cord.[25] Plasticity of spared tracts and behavioral substitution often allow spontaneous respiratory, motor[26–28] and sensory recovery.[29]

Several investigators have hemisected[30,31] or crushed[32] part of the lumbosacral cord to study pain after SCI. Faulkner and colleagues[33] stabbed and crushed the L1-L2 spinal cord in mice to investigate the protective effect of reactive astrocytes. Fukuda and colleagues[34] developed a lumbar SCI model in dogs by inflating a balloon catheter in the vertebral L1 spinal canal. Shunmugavel and colleagues[35] developed a cauda equina compression model in rats by implanting silicone gels into L4 and L6 vertebral epidural spaces. Finally, Magnuson and colleagues[36] found severe locomotor deficits after contusions of the T13-L1 and L1-L2 spinal cord and less severe locomotor deficits after contusions of the L3-L4 spinal cord. Lower lumbosacral spinal cord injuries do not severely compromise locomotion in rats.[37]

We describe a rat lumbosacral spinal cord contusion model with reproducible anatomical, histological, and functional outcomes similar to human lumbosacral injuries. Motoneuronal pools for lower limb muscles are situated in L4-L5 spinal cord located in the T13 and L1 vertebral canal. To assess spinal cord damage resulting from a 25 mm or 50 mm weight drop contusion, we counted motoneurons identified by backfilling the tibial and common peroneal nerves with fluorescent dyes, quantified spared white matter, determined diameters of myelinated axon and thickness of myelin sheath in the two nerves, and assessed atrophy of the tibialis anterior and gastrocnemius muscles. To assess functional deficits, we used static and walking footprint analysis.

Contusion of the rat spinal cord at T13-L1 vertebral junction with a 10 g weight dropped from a height of 25 or 50 mm resulted in graded lumbosacral SCI accompanied by reproducible graded tibial and peroneal motoneuronal losses, white matter losses, peripheral nerve axonal diameter decrease, reduced myelinated axonal thickness, and atrophy of the tibialis anterior (TA) and gastrocnemius (GA) muscles, as well as easily measurable changes in both static and walking footprints of the rats. This model can be used to assess regenerative therapies of lumbosacral SCI, including motoneuronal replacement and reinnervation of muscle.

Methods

Animals, care, and euthanasia

Three green fluorescent protein (GFP)–expressing Sprague-Dawley female rats (10 weeks) were obtained from the W. M. Keck Center for Collaborative Neuroscience for preliminary studies of the anatomy of the lumbosacral cord and distribution of tibial and peroneal motoneurons. A total of 26 wild-type adult female Sprague-Dawley rats (10 weeks old, 210–230 g) were purchased from Charles River Laboratory for the lumbosacral SCI experiments. The rats were randomized to three injury groups: Sham (laminectomy only, $n = 9$); 25 mm spinal cord contusion ($n = 8$); and 50 mm spinal cord contusion ($n = 9$).

The rats were housed in a controlled environment room, and provided with standard rodent chow and water for a week before the study. The rats were maintained in individual rat boxes for six weeks, received bladder expression one to two times daily, and assessed before and weekly after surgery for standing and walking footprints. The rats were euthanized and fixed by perfusion at six to seven weeks. The experimental protocol complies with Rutgers and National Institutes of Health regulations regarding protection of animals used for experimental purposes. The Rutgers Animal Care and Facilities Committee (the equivalent of the institutional animal care and use committee) approved the protocol.

For surgical procedures, the rats were deeply anesthetized with isoflurane (5% induction and 1–2% maintenance). For euthanasia and fixation, the rats were deeply anesthetized with intraperitoneal injections of ketamine (80 mg/kg) and xylazine (10 mg/kg). To fix the rats for histology, we opened the chest cavity, inserted a blunt needle through the left ventricle into the aorta, clamped the needle in place, and cut open the right atrium. After injecting one mL of 1% lidocaine to dilate blood vessels, we perfused 200 mL of saline at 35 mL/min to wash out blood, and then 300 mL of 4% paraformaldehyde at 25 mL/min.

Retrograde motoneuronal labeling

Three transgenic GFP (green-fluorescent-protein) expressing Sprague-Dawley rats and twelve wild-type Sprague-Dawley rats were euthanized seven weeks after SCI. At six weeks after injury, we applied Fluoro-Ruby (FR, Invitrogen, NY) and Fluoro-Gold (FG, Fluorochrome, CO) dyes to the common peroneal and tibial nerves to label motoneurons innervating the nerves. We anesthetized the rats with isoflurane, incised the back of the thigh and knee, blunt-dissected muscles to expose the tibial nerve and common peroneal nerves, cut the nerves with sharp scissors, placed the proximal stumps into small polyethylene tubes containing 2% dye (FR or FG) in saline, sealed the tubes with silicone grease and Vaseline to prevent leakage, and left the tracer in contact with the nerve for at least 1 h. The tube was then removed, the nerve was rinsed in saline, and the skin was sutured.

One week later, the rats were anesthetized, perfused, and fixed as described above. The spinal cord were removed, placed in the 30% sucrose/0.1 M phosphate buffer at 4°C for 24 h, and embedded in OCT compound (Fisher, Pittsburgh, PA). Serial sagittal sections were cut at a thickness of 50 μm using a cryostat microtome

(OTF5000, Bright instrument Co Ltd., Cambridgeshire, UK), washed three times with 0.1 M PBS and cover-slipped with fluorescence-compatible anti-fade mount (Mo1, Biomedia, CA). We imaged sections with an epifluorescent microscope (Axiovert 200M, Zeiss, Germany) and counted FR- and FG-positive motor neurons in all sections using ImageJ software.

The L5 to S1 spinal cord segments are located just above and below the junction of T13 and L1 vertebrae. The dorsal root entry zones for L4 and L5 roots were on either side of the junction. The tibial nerve (L4-5, S1-S3) gives off branches to the gastrocnemius, popliteus, soleus, and plantaris muscles, as well as the sensory sural nerve that innervate the lateral foot. The common peroneal nerve (L4-5, S1-2) form the superficial and deep peroneal nerves, innervating the peroneus longus, peroneus brevis, and short head of the biceps femoris muscles.

Lumbosacral spinal cord contusion

We anesthetized rats with isoflurane (5% induction and 1–2% maintenance) using a facemask, shaved the rats, washed the skin with betadine solution, and surgically exposed the L1 dorsal process. After removing the dorsal lamina of L1, we placed a suture to mark the lower margin of T13, and then removed the T13 dorsal lamina. The Sham group received only laminectomy.

The MASCIS Impactor (Multicenter Animal SCI Impactor, W.M. Keck Center for Collaborative Neuroscience, Piscataway, NJ) was used to drop a 10 g rod (impactor head diameter, 2.5 mm) from a height of either 25 mm or 50 mm onto the spinal cord at the junction of T13 and L1 vertebral bodies. The dura was not opened. After contusion, we placed a piece of subcutaneous fat on the dural surface to prevent adhesions between the dura and surrounding tissues.

After injury, we manually expressed the bladders of the rats twice daily for a week and once daily as necessary after the first week, injected 6 mL saline subcutaneously daily for 3 d, and gave antibiotics (Cefazolin 50 mg/kg) subcutaneously daily for one week. After the first week, if the rats showed evidence of urinary tract infection (i.e., hemorrhagic and cloudy urine), they were housed separately from the other rats and given subcutaneous enrofloxacin (Baytril 2.5 mg/kg per day) daily for 10 d. If the urinary tract infection had not resolved within that period, the rats would have been euthanized. None were.

If the rats had shown signs of post-operative pain during the first week after surgery, we would have been treated with buprenorphine (0.05 mg/kg) subcutaneously daily. None did. Animals that showed early signs of autophagia or autotomy, they would receive oral acetaminophen (64 mg/kg, Infant TYLENOL® Oral Suspension Liquid; Johnson & Johnson, New Brunswick, NJ) daily for the remainder of the experiment. The rats readily drank the medicine from a dropper. Two rats did not respond and were euthanized, one from the 25 mm and the other from 50 mm injury group.

Footprint analyses

The rats were assessed before injury (Day 0) and tested weekly for changes in their walking and standing footprints. To obtain walking footprints, the rats were placed in a confined walkway that has a dark shelter at the end of the corridor (10 × 100 cm). White paper was placed on the walkway. The hind paws of the rats were inked with a paint-soaked sponge. As they walked down the corridor, they left their footprints on the paper. The rats were trained to walk in the corridor and baseline-walking tracks were recorded before surgery.

Three measurements were made from the walking footprints: Footprint Length (FL) distance is the change in footprint length from the heel to the third toe before injury (NFL) to after injury (EFL) divided by NFL; therefore, (EFL-NFL)/NFL. Toe Spread (TS) is the change in distance from the first to the fifth toe before (NTS) and after injury (ETS), divided by NTS; therefore, (ETS-NTS)/NTS. Intermediate Toe Spread (ITS) is the change in distance from the second to the fourth toe before (NITS) and after (EITS), divided by NITS.

Table 1. Distances (μm) of Farthest Labeled Motoneurons From T13-L1

	Proximal end	*Distal end*
Tibial nerve	1772.0 ± 199.1	2939.3 ± 314.3
Common peroneal nerve	2411.7 ± 323.9	2601.7 ± 339.0

The ± values indicate standard deviation.

These measurements were used to calculate the sciatic function index (SFI) proposed by Bain and colleagues[38] and described in Table 2. An SFI index is set at −100 if no footprint were measurable (i.e. the rats could not walk).[39,40] In cases where the rat could not walk, we assumed 45 mm for FL (39.1 mm is the longest observed), 10 mm for TS (10.1 mm was the shortest observed), and 5.0 mm for ITS (5.3 mm was the shortest observed).

For standing or static footprints, the rats were placed into acrylic glass containers (25 cm × 15 cm × 10 cm) on a transparent base plate and photographed from below. We analyzed five photographs of each rat by ImageJ. Toe spread factor (TSF) is the distance between the first and fifth toes on standing footprints. Intermediate toe spread factor (ITSF) is the distance from the second to the fourth toe. The SSI[41] was calculated from TSF and ITSF, as described in Table 2.

Fixation, sectioning, and staining

At six weeks after injury, animals were anesthetized and perfused transcardially with 0.9% saline and then 4% paraformaldehyde. The spinal cords, tibial nerve, common peroneal nerve, tibialis anterior (TA) and gastrocnemius (GA) were collected and post-fixed in 4% paraformaldehyde for 24 h. For spinal cord sections, we cut 1-cm lengths of spinal cord centered on the injury area, serially sectioned the cord horizontally, and stained two sections from every 20 sections, one for Luxol Fast Blue (LFB) and the other for NeuN staining.

Fixed tissues were dehydrated through a graded series of ethanol solutions, cleared in xylene, and embedded in paraffin blocks for sectioning. Spinal cord sections were cut with a rotary microtome (Model 820, American Optical, NY) at 5 μm thickness and mounted on slides. The sections were deparaffinized in xylene and rehydrated in 100% and then 95% ethanol. The sections were then stained with LFB for myelin or NeuN antibody for neurons.

To stain white matter, we incubated sections in 0.1% Luxol Fast Blue (LFB, Acros, NJ) diluted in 95% ethanol with 10% acetic acid

Table 2. Footprint Factors

Factors	*Calculation*
Footprint length factor (FLF)	FLF = (EFL - NFL) / NFL
Toe spread factor (TSF)	TSF = (ETS - NTS) / NTS
Intermediate toe spread factor (ITSF)	ITSF = (EITS - NITS) / NITS
Sciatic Function Index (SFI)	SFI = −38.3 × FLF + 109.5 × TSF + 13.3 × ITSF − 8.8
Static Sciatic Index (SSI)	SSI = 108.44 × TSF + 31.85 × ITSF − 5.49

EFL, footprint length after injury; NFL, footprint length before injury; ETS, toe spread after injury; NTS, toe spread before injury; EITS, intermediary toe spread after injury; NITS, intermediary toe spread before injury.

at 56°C for 24 h, rinsed in 95% ethanol and then distilled water, differentiated in 0.05% lithium carbonate, rinsed in 70% ethanol, dehydrated in 99% ethanol, cleared with xylene, and cover-slipped with mounting media. LFB-stained sections were photographed with a microscope (Axiophot, Zeiss, Germany). Areas of spared white matter were outlined and quantified (ImageJ) every 20th section. Sections with the least spared white matter were designated the injury epicenter.

For NeuN staining, we first did antigen retrieval by immersing sections in fresh citrate buffer (1 g NaOH, 2.1 g citric acid, and 1 L H_2O), heating for 15 min at 100°C, and cooling at room temperature for 20 min. The sections were incubated in primary antibody for NeuN (1:1000 dilution; Millipore, MA) overnight at 4°C, washed with PBS, incubated in biotinylated secondary antibody (1:500 dilution; Millipore) for 1 h at room temperature, followed by ABC (avidin and biotinylated horseradish peroxidase; Vector, CA) and DAB (3,3′-diaminobenzidine), washed and then cover-slipped with mounting medium.

The tibial nerves and common peroneal nerves were mounted in paraffin, cut into 5-μm cross-sections, and stained with Holmes Silver Nitrate and LFB. Briefly, sections were deparaffinized and hydrated to distilled water, placed in 20% silver nitrate in dark at room temperature for 1h, washed in water, placed in impregnating solution at 37°C overnight, placed in reducing solution for 5 min, washed in distilled water, toned in 0.2% aqueous gold chloride for 3 min, placed in 2% aqueous oxalic acid for 5 min, placed in 5% aqueous sodium thiosulfate, and washed in tap water for 10 min, followed by LFB staining.

Image analyses

Spinal cord sections were photographed with an epifluorescent microscope (Axiophot). Motor neuronal cell bodies in ventral horn were outlined using ImageJ software. Ventral horn was defined as gray matter ventral to the central canal. Only motor neurons with a clearly identifiable nucleus and a cell soma larger than 100 μm^2 were counted. Motor neurons were counted every 20th section. (Please note that these counts do not represent total motoneuron count and is a sampling approach.)

Sections of the peripheral nerves were digitally photographed with a microscope (Axiophot). Total numbers of myelinated axon were counted manually from representative images while axon diameter and thickness of myelin sheath were determined with ImageJ software. We calculated mean axon numbers, axon diameters, and thickness of myelinated sheaths, with standard error of means for the three groups.

To quantify muscle atrophy, we cut thin (5 μm) cross-sections of TA and GA muscles, stained the sections with hematoxylin and eosin (H&E), and digitally photographed the sections with a microscope (Axiophot). On each image, two vertical and five horizontal lines were drawn. One muscle fiber close to the intersection of a vertical and horizontal line was selected for analysis. A total of 10 muscle fiber cross-sectional areas (CSA, expressed in square micrometers) were determined with the ImageJ program from representative sections from each animal. We calculated mean fiber CSA and standard errors of means for each injury group (Sham, 25 mm, and 50 mm).

Statistics and number of animals studied

Results are expressed as means ± standard deviation. We used a commercial statistics program (Statview) to do analysis of variance (ANOVA) to estimate overall statistical significance and a post hoc test (Scheffe's test) to estimate statistical significance of differences between pairs of groups. To assess change of footprint parameters over time, we used repeated ANOVA (over time) and a post hoc test (Scheffe's test) to determine the effects of time on each variable. Some data were expressed as a percentage of controls. For example, white matter areas are expressed as a percentage of mean value of the Sham group. A p value of less than 0.05 was considered statistically significant.

Some preliminary experiments were excluded from this report. In preliminary studies (unpublished) using several male Sprague-Dawley rats, we found that male rats developed flaccid bladders and had bladder blood clots after a 50 mm L4-L5 spinal cord contusion. We limited further experiments to female rats and excluded the male results.

A total of 29 female rats were studied. Three rats were not injured and studied for distribution of back-labeled peroneal and tibial motoneurons. The remaining 26 rats were randomized to three injury groups (i.e., Sham, $n=9$; 25 mm, $n=8$; and 50 mm, $n=9$). One rat in the 25 mm group and one rat in the 50 mm group had to be euthanized and perfused two weeks after surgery due to autotomy (self-amputation of digits or foot). One rat in the 50 mm group showed a mild heel ulcer in the sixth week after surgery but the condition was well controlled with acetaminophen. One rat in the Sham group died during the procedure to label motoneurons. The footprint and spinal cord histological data came from 23 rats (i.e., eight rats in the Sham group, seven rats in the 25 mm group, and eight rats in the 50 mm group). Twelve of the 23 rats were studied with retrograde labeling of the peroneal and tibial nerves in horizontally sectioned spinal cords (four Sham, four 25 mm, and four 50 mm). The 11 remaining rats were studied with coronal sections of the spinal cord, peripheral nerve, and muscle histology (four Sham, three 25 mm, and four 50 mm).

Results

Determination of injury site

We chose the injury site based on the following reasons. First, we wanted to identify an unambiguous landmark that could be used to direct the contusion. The junction of the T13 and L1 vertebra is a distinct landmark that could be easily identified. Second, our goal was to injure motoneurons from the tibial nerve and common peroneal nerves. We therefore identified motoneuronal pools of these two nerves by backfilling with fluorescent dyes and then contused the spinal cord where these motoneurons were located. Third, we wanted to avoid the L2 spinal cord where the central pattern generator (CPG) is located.

We used three GFP Sprague-Dawley rats to identify locations of tibial and common peroneal motoneuron pools (GFP Sprague-Dawley rats express green fluorescent protein so that the sections were fluorescent green). We backfilled tibial and common peroneal nerves with Fluoro-Gold (blue fluorescence) and Fluoro-Ruby (reddish orange fluorescence). To expose the T13-L1 junction, we did a laminectomy of L1 (Fig. 1A), marked the lower edge of T13 (indicated by dashed line in Fig. 1B) with a suture at the laminectomy edge, cut the spinal cord with a sharp scalpel, and then removed the lamina of T13. Figure 1 shows a horizontal section of the spinal cord with a cut at the lower edge of T13.

The tibial and common peroneal motoneurons were clearly visible even in low-power views of the section. The lengths of the motor columns were 4.71 mm for the common peroneal nerve and 5.01 mm for the tibial nerve. Table 1 lists the mean distances of the most proximal and distal labeled neurons from the T13/L1 vertebral junction. Motoneuron pools of common peroneal and tibial nerves overlapped with each other. Motoneurons of tibial nerve were more caudal and lateral than common peroneal motoneurons. The center of the common peroneal motoneuronal column was close to junction of the T13/L1 vertebra while the center of the tibial motoneuronal column was about 500 μm distal to the T13/L1 vertebral junction. Contusion of the spinal cord at the T13/L1 vertebral

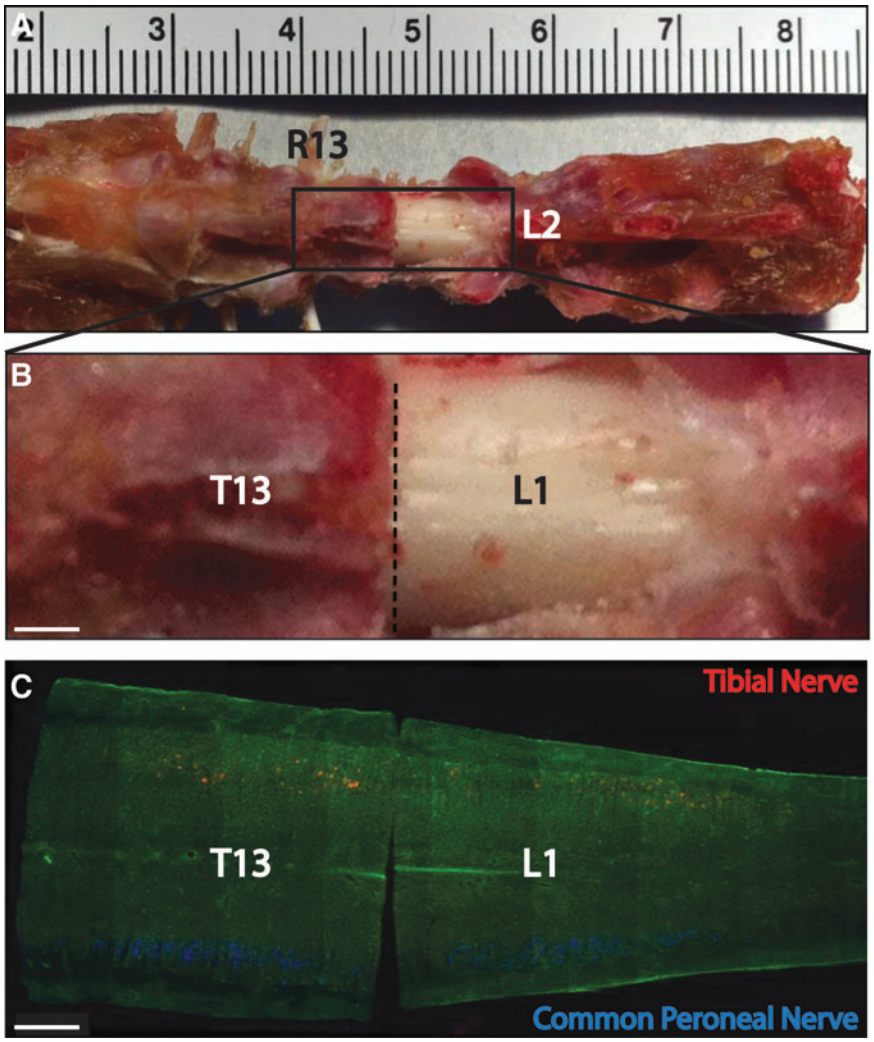

FIG. 1. Retrograde labeling of tibial and common peroneal nerve, and anatomy of rat's spine and spinal cord. **(A)** Anatomy of rat's spine and spinal cord, exposed by a L1 laminectomy. **(B)** Enlarged box area in A. The lower margin of T13 laminae is indicated by a dashed line. **(C)** Motoneurons labeled by fluororuby (red) and fluorogold (blue) backfilled respectively from the tibial nerve and common peroneal nerve by retrograde labeling. The spinal cord cut between T13 and L1. R13, rib 13; T13, vertebra T13; L1, L1 vertebra; L2, L2 vertebra. Scale bar, 500 μm.

junction should damage both the common peroneal and tibial motoneuron pools.

Walking footprints

Before injury, mean FLs were 20.1 ± 0.95 mm, 23.04 ± 1.26 mm, and 22.38 ± 1.57 mm for the Sham, 25 mm, and 50 mm groups, respectively. Normally, rats walked with their heels elevated from the ground. After injury, as shown in Figure 2H, the rats walked with their heels on the ground and hence had longer footprints. At one week after injury, three of seven rats in Group 25 mm and four of eight rats in Group 50 mm could not take steps and their footprint lengths were assumed to be 45 mm. With these assumed values, mean footprint lengths of the 25 mm and 50 mm groups, respectively, increased to 39.89 ± 5.88 mm and 40.33 ± 5.07 mm (Fig. 2). By two weeks, all the rats were able to walk. Repeated ANOVA indicated significant differences among the groups ($p < 0.0001$). Post hoc testing revealed significant differences between the Sham and 25 mm groups ($p < 0.0001$), the Sham and 50 mm groups ($p < 0.0001$), and the 25 mm and 50 mm groups ($p = 0.0023$).

TS and ITS decreased after SCI (Fig. 2). Before injury, TS was approximately 20 mm and ITS was approximately 11 mm. One week after T13/L1 injury, TS decreased to 12.30 ± 2.84 mm and 10.51 ± 0.79 mm in the 25 mm and 50 mm groups, respectively; ITS decreased to 7.39 ± 2.34 mm and 5.76 ± 1.01 mm, respectively. Both TS and ITS partly recovered at two to six weeks. ANOVA indicated significant differences of TS ($p < 0.0001$) and ITS ($p < 0.0001$) among the groups. Post hoc testing showed significant differences in TS ($p < 0.0001$) and ITS ($p = 0.0028$) between Sham and 25 mm, TS ($p < 0.0001$) and ITS ($p < 0.0001$) between Sham and 50 mm, and TS ($p = 0.0018$) and ITS ($p = 0.0006$) between 25 mm and 50 mm.

The SFI decreased precipitously to -83.04 ± 24.19 and -93.51 ± 8.65 in the 25 mm and 50 mm groups one week after injury while it remained stable between 0 and -10 in the Sham group (Fig. 2). SFI in the 25 mm and 50 mm groups recovered gradually to -54.29 ± 8.74 and -68.57 ± 9.12 respectively after six weeks. From weeks one to six, mean SFI of the 25 mm group was higher than the 50 mm group. ANOVA indicated significant differences among these three groups ($p < 0.0001$). Post hoc testing reveal significant differences between the Sham and 25 mm groups

($p < 0.0001$), the Sham and 50 mm groups ($p < 0.0001$), and the 25 mm and 50 mm groups ($p < 0.0001$).

Static footprints

We analyzed standing or static footprints of the rats by photographing the feet of the rats standing on a transparent acrylic platform. Normally, rats spread their toes when they stand (Fig. 3A) so that the distances between the first and last toes (static toe spread or STS) are ~20 mm and the distances between the second and fourth toes (static intermediate toe spread or SITS) are ~12 mm (Fig. 3A).

One week after T13/L1 injury, STS decreased to 10.94 ± 3.09 mm and 8.79 ± 2.10 mm in Group 25 mm and 50 mm, respectively. SITS decreased to 7.27 ± 1.48 mm and 5.91 ± 1.07 mm, respectively. Both STS and SITS gradually increased at two to six weeks after SCI but they all were significantly lower than the Sham group at six weeks. ANOVA indicated significant differences among the three groups both for STS ($p < 0.0001$) and SITS ($p = 0.0001$). Post hoc testing revealed significant differences between Sham and 25 mm in STS ($p = 0.001$) and SITS ($p = 0.0066$), Sham and 50 mm in STS ($p < 0.0001$) and SITS ($p = 0.0001$), and 25 mm and 50 mm in STS ($p = 0.0363$). However, there was no difference in SITS between the 25 mm and 50 mm groups ($p = 0.1983$).

SSI fell precipitously to -67.84 ± 22.26 and -83.70 ± 13.88 in the 25 mm and 50 mm groups, respectively, one week after injury while SSI in the Sham group was stable (Fig. 3). SSI in Group 25 mm and Group 50 mm increased gradually to -39.66 ± 19.58 and -73.80 ± 16.19 after six weeks, respectively. From weeks one to six, SSI values of Group 25 mm were always higher than Group 50 mm, consistent with more severe injury in Group 50 mm rats than in Group 25 mm rats. ANOVA indicated significant difference among these three groups ($p < 0.0001$). Post hoc testing reveal significant differences between the Sham and 25 mm groups ($p = 0.0029$), the Sham and 50 mm groups ($p < 0.0001$), and the 25 mm and 50 mm groups ($p = 0.0220$). Although the SSI scores were statistically significant in the three injury groups, the standard errors of means were much greater than the SFI score and the p values were correspondingly greater, particularly between the 25 mm and 50 mm groups.

Motoneuron loss

To assess motoneuronal loss, we counted NeuN-stained cells that met the criteria for motoneurons in coronal sections (i.e., located in ventral horn) with a clearly identifiable nucleus and a cell soma larger than 100 μm^2 (Fig. 4). In the Sham group, the number of motoneurons declined from 20–25/section at the T13 vertebral level to 15–20/section at the L1 vertebra level. Injury caused complete loss of motoneurons at the lesion epicenter (Fig. 4C), gradually returning to levels similar to the Sham group at 5 mm rostral and caudal. Repeated measures ANOVA indicated significant difference of spared motoneurons among the three injury groups ($p < 0.0001$). Post hoc testing revealed significant differences between Groups Sham and 25 mm ($p < 0.0001$), Groups Sham and 50 mm ($p < 0.0001$); and Groups 25 mm and 50 mm ($p = 0.0004$).

To identify loss of specific motoneuronal groups, we used Fluoro-Ruby (FR) and Fluoro-Gold (FG) to identify the tibial and peroneal motoneuron pools. FR usually produces a reddish fluorescence while FG tends to be bluish. Figure 5 shows FR and FG labeled motoneurons back-labeled from the tibial nerve and common peroneal nerve. Figure 5A to 5C are pictures with all motoneurons from one animal projected on one spinal cord background. Figure 5D to 5F are hand-drawn (camera lucida) pictures corresponding to Figure 5A to 5C. All labeled neurons were located in gray matter and exhibited morphology consistent with motoneurons. The cells have large multipolar perikarya with several dendrites that extended radially from the cell body.

Before injury, mean motoneuronal counts were 931.7 ± 25.11 backfilled from the tibial nerve and 944.7 ± 20.11 backfilled from the peroneal nerve. After T13/L1 contusions, the numbers of spare motoneurons fell precipitously. In the 25 mm group, the motoneuron count was 546.5 ± 144.96 for tibial nerve and 542.0 ± 11.37 for peroneal nerve (i.e., about half of the motoneurons were destroyed). In Group 50 mm, the counts were 327.0 ± 87.23 for tibial nerve and 294.0 ± 57.37 for peroneal nerve (i.e. about two third of the back-labeled motoneurons were destroyed).

Spared white matter in spinal cord

The contusions spared consistent white matter areas at the injury site. Figure 6 shows Fast Blue–stained white matter of a 10 mm length of the spinal cord at impact center six weeks after surgery. Total coronal spinal cord areas, as well as white matter (blue stained) areas, were lower in the injured spinal cords. We calculated percentages of spared white matter by dividing the number of blue pixels in injured cord sections by the mean number of pixels of white matter areas in the Sham group.

Compared with the Sham group, both the 25 mm and the 50 mm groups showed significant loss of white matter at distances up to 5 mm from the lesion epicenter. The 50 mm group had significantly less spared white matter than the 25 mm group. Repeated ANOVA indicated significant difference of spare white matter among the three groups ($p < 0.0001$). Post hoc testing revealed significant differences of spared white matter between the Sham and 25 mm groups ($p < 0.001$), the Sham and 50 mm groups ($p < 0.0001$), and the 25 mm and 50 mm groups ($p = 0.0147$).

The pattern of white matter sparing is different from thoracic spinal cord injuries where a rim of white matter usually is present both in the dorsal and ventral regions. In the lumbosacral spinal cord, the spared white matter was largely present in the ventral region and absent from the dorsal region after a 25 mm weight drop contusion. After spinal cords injured with the 50 mm weight drop, there was

FIG. 2. Walking footprint and analysis. **(A–C)** Pictures of typical footprints obtained at one week after injury in the Sham, 25 mm, and 50 mm groups, respectively. Scale bar (A-C), 10 mm. Dash line: Footprint length (FL), maximum distance from the third toe to end of the print; Toe spread (TS), distance between the first and fifth toes; Intermediate toe spread (ITS), distance from the second to the fourth toe. **(D)** The increase in mean footprint length (FL) in the Sham ($n = 8$), 25 mm ($n = 7$), and 50 mm ($n = 8$) groups. **(E)** and **(F)** show the decrease in toe spread (TS) and intermediate toe spread (ITS) in the three injury groups. **(G)** shows the decrease in mean sciatic function index (SFI) scores. The error bars indicate standard deviation. The three groups differed significantly from each other at all time-points after the first week. * indicates significant difference compared with the Sham group. # indicates significant difference between 25 mm and 50 mm groups. **(H)** shows a walking injured rat (2 weeks after injury) while **(I)** shows a normal rat. Both rats had just moved their left hindlimb forward. The heel of injured rat (H red arrow) touched the ground, while normal one did not. The toes of injured rat (H blue arrow) did not flatten and spread, while the normal one did. Neither of these behaviors would be rated in a BBB score.

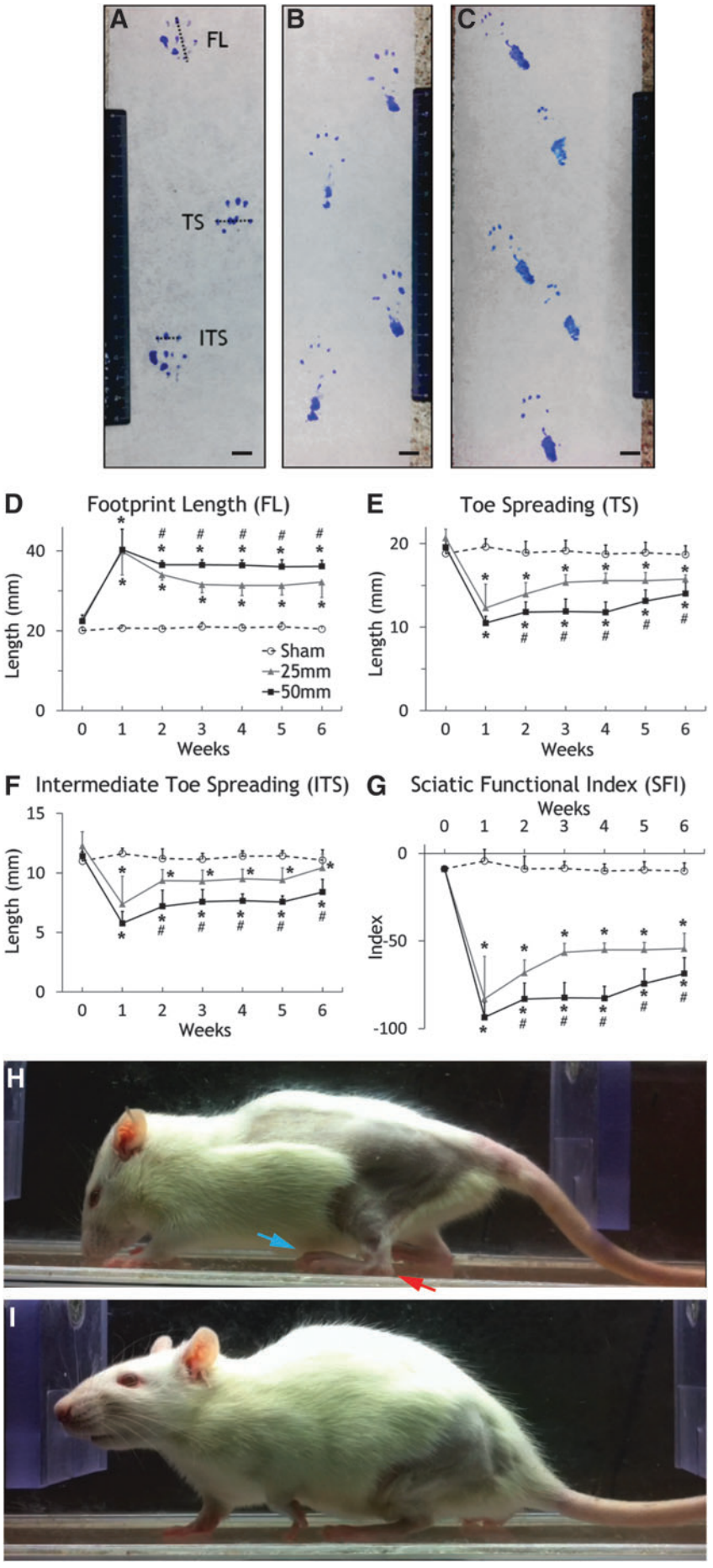
A
FL
TS
ITS
B
C
D
Footprint Length (FL)
Length (mm)
Weeks
Sham
25mm
50mm
E
Toe Spreading (TS)
Length (mm)
Weeks
F
Intermediate Toe Spreading (ITS)
Length (mm)
Weeks
G
Sciatic Functional Index (SFI)
Weeks
Index
H
I

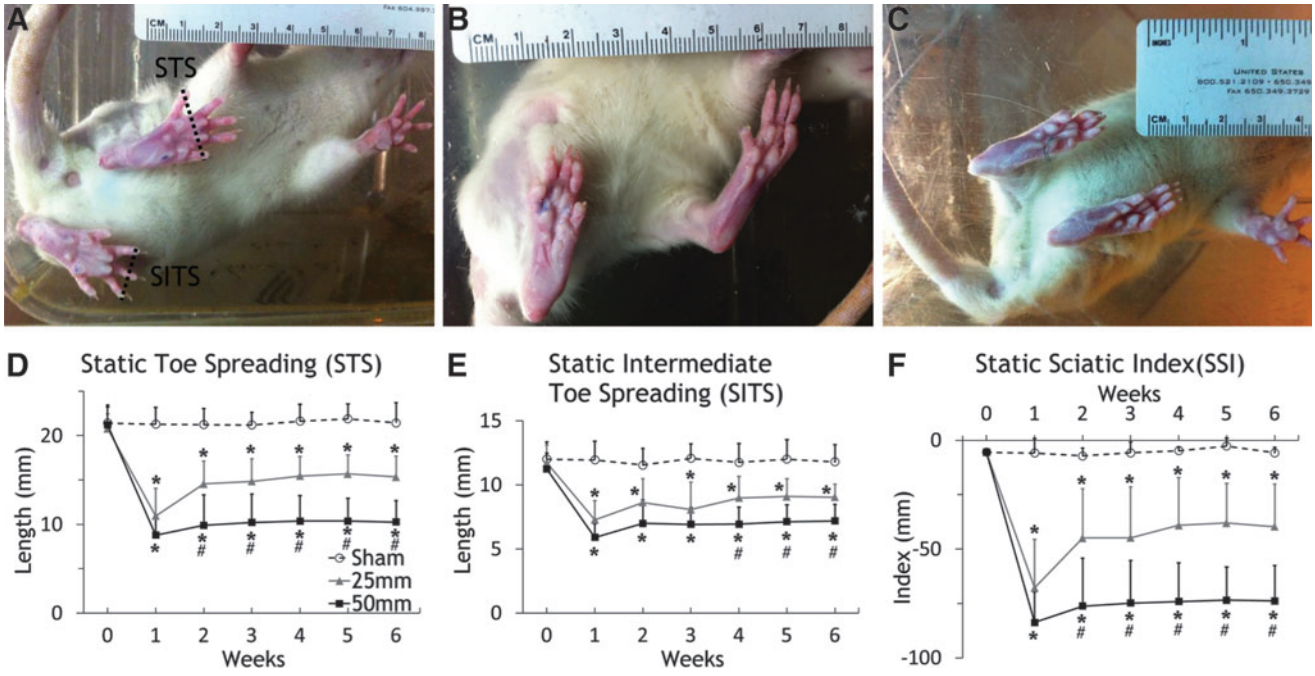

FIG. 3. Static foot positions and analysis. **(A–C)** Images of typical foot positions at two weeks after injury in the Sham, 25 mm, and 50 mm groups, respectively. **(D)** and **(E)** show the declines in mean static toe spreading (STS) and static intermediate toe spreading (SITS) in the three injury groups. **(F)** shows the declines of Static Sciatic Index scores in the three injury groups. The error bars indicate standard deviation. Animal numbers are the same as in Figure 2. All changes of foot positioning scores were statistically different among the three injury groups after the third week. * indicates significant difference compared with the Sham group. # indicates significant difference between the 25 mm and 50 mm groups.

significantly less and often no white matter left at the epicenter. Only a few LFB-stained patches were present in the lateral area.

Axonal changes in common peroneal and tibial nerves

We assessed axons in the tibial and common peroneal nerves (Fig. 7). Profiles of collapsed axons surrounded by myelin sheaths were present in both nerves of rats injured by 25 mm or 50 mm contusions (Fig.7F, 7G). Total myelinated axon counts in tibial nerve were 3015.2 ± 180.0 for the Sham group, 2939.4 ± 144.1 for the 25 mm group, and 2852 ± 145.7 for 50 mm group. Total myelinated axonal numbers in common peroneal nerve was 1007.6 ± 133.6 for the Sham group, 967.4 ± 88.3 for the 25 mm group, and 994.4 ± 119.3 for the 50 mm group. ANOVA showed no significant differences of total myelinated axon numbers among the three groups ($p > 0.05$) in either nerve.

Axon diameters, however, decreased significantly after surgery. In the Sham group, mean axon diameters were $2.54 \pm 0.49\ \mu$m for tibial nerve and $2.38 \pm 0.32\ \mu$m for peroneal nerve. In the 25 mm group, it fell to $1.74 \pm 0.59\ \mu$m and $1.89 \pm 0.44\ \mu$m, respectively. In the 50 mm group, it was $1.41 \pm 0.40\ \mu$m and $1.41 \pm 0.19\ \mu$m, respectively. ANOVA revealed significant differences among three groups for both nerves ($p < 0.0001$). For tibial nerves, Scheffe's post hoc tests indicated significant differences between Sham and 25 mm ($p = 0.005$), Sham and 50 mm ($p = 0.0001$), but not for 25 mm and 50 mm ($p = 0.3601$). For peroneal nerves, Sham and 25 mm ($p = 0.0098$), Sham and 50 mm ($p < 0.0001$), and 25 mm and 50 mm ($p = 0.0135$) differed significantly.

Myelin thickness also decreased significantly after surgery. In the Sham group, myelin thickness averaged $2.22 \pm 0.23\ \mu$m for tibial nerve and $2.29 \pm 0.33\ \mu$m for peroneal nerve. In the 25 mm group, the mean myelin thickness was $1.59 \pm 0.21\ \mu$m, and $1.84 \pm 0.39\ \mu$m, respectively. In the 50 mm group, the mean myelin thickness was $1.18 \pm 0.31\ \mu$m, and $1.24 \pm 0.268\ \mu$m, respectively. ANOVA indicated significant differences among the groups for both nerves ($p < 0.0001$). Scheffe's post hoc testing revealed significant differences of tibial myelin thickness between Sham and 25 mm ($p < 0.0001$), Sham and 50 mm ($p < 0.0001$), and 25 mm and 50 mm ($p = 0.0051$) for the tibial nerve. Likewise, 25 mm ($p = 0.0166$) and 50 mm ($p < 0.0001$) groups differed significantly from Sham and each other ($p = 0.0014$).

Histologic examination of TA and GA muscle

Both the tibialis anterior (TA) and gastrocnemius (GA) muscles showed evidence on atrophic changes on hematoxylin & eosin staining. Muscles were transversely sectioned to show cross-sections of muscle fibers. Injury clearly reduced muscle fiber size. To quantify the atrophy, we analyzed three sections of each muscle sample from the Sham ($n = 3$), 25 mm ($n = 4$), and 50 mm ($n = 4$) groups. On each section, five images were obtained. In each image, we measured the cross-sectional areas (CSA) of 10 randomly-chosen fibers.

Figure 8 shows the histologic changes of GA muscle in the three groups. Injury clearly changed the appearance of the muscle. In the Sham group, the muscle fibers were large and pinkish with eccentric nuclei and CSA of 1300–1500 μm2. Muscle fiber CSA's in the GA muscle were slightly bigger than in the TA muscle. Injury remarkably reduced the CSA of the muscle fibers. After 25 mm contusion of the spinal cord, hematoxylin and eosin-stained muscles fibers were smaller and deeper purple, with large trabeculae separating bundles of shrunken muscle fibers. After 50 mm contusions of the spinal cord, the muscle fibers were even smaller and more condensed.

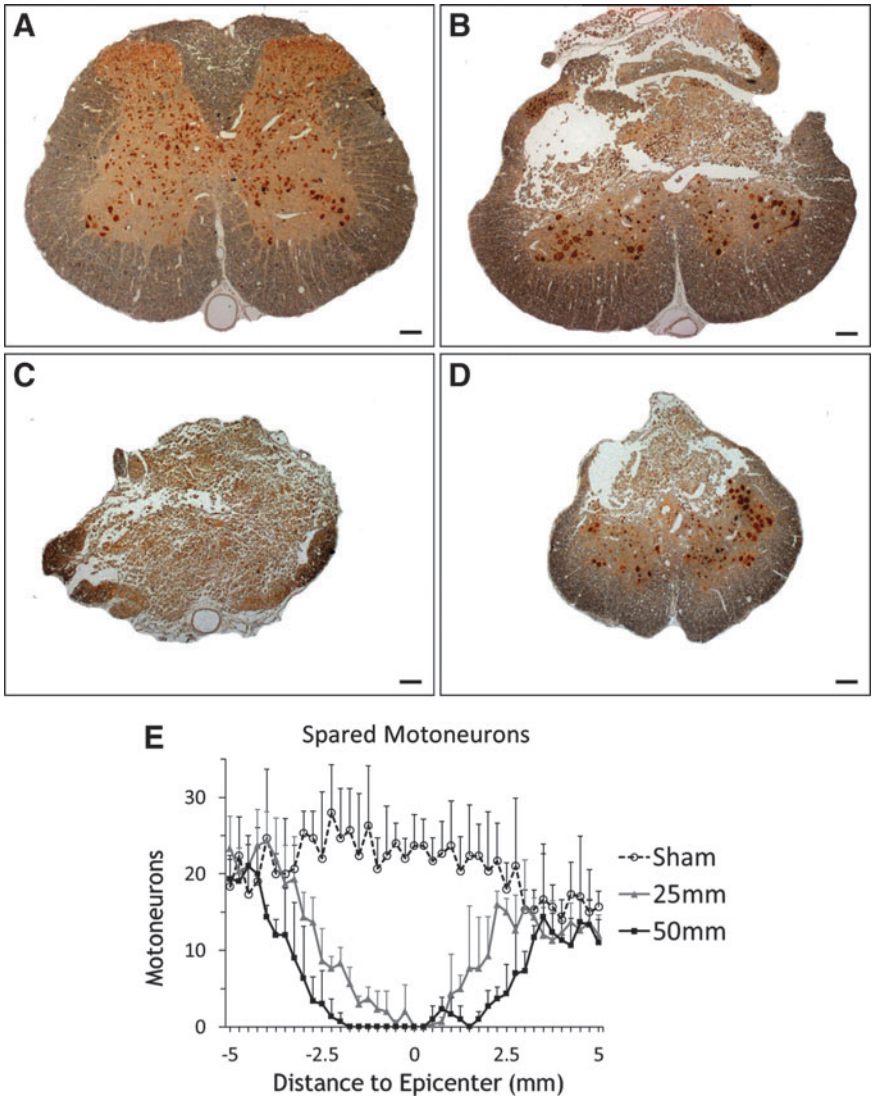

FIG. 4. Counts of spared NeuN-stained motoneurons. **(A)** Normal spinal cord. Large motoneurons are located in the ventral horn. **(B)** Injured spinal cord in Group 50 mm about 3 mm proximal to injury epicenter. **(C)** Injury epicenter in Group 50 mm. **(D)** Injured spinal cord in Group 50 mm about 3 mm distal to injury epicenter. Scale bar (A-D), 200 μm. **(E)** Graph of the numbers of spare motoneurons of ± 5 mm of the injury epicenter in the Sham ($n=4$), 25 mm ($n=3$), and 50 mm ($n=4$) injury groups. The error bars indicate standard deviation.

The muscle atrophy was not only visually apparent but also remarkably different among the three groups when quantified. Measurements of muscle fiber CSA indicate that a 25-mm contusion of the L4-5 spinal cord reduced CSA by nearly 40% in both the GA and TA. A 50-mm contusion reduced CSA by nearly 80%. ANOVA indicated significant differences among the injury groups and post hoc testing indicated that 25 mm and 50 mm differed significantly from Sham, as well as each other ($p<0.05$). These changes are not only consistent with atrophy of the muscles due to the SCI but suggest that measurement of muscle fiber CSA may provide a sensitive measure of injury severity and possible recovery of function.

Discussion

In humans, injuries to the lumbosacral spinal cord at the T12/L1 vertebral segments usually cause flaccid paralysis of the lower limb muscles that control the foot, including the gastrocnemius and anterior tibialis. In addition, such injuries cause paralysis of the pelvic organs, including the bladder and anal sphincter, as well as loss of sexual function. Lumbosacral SCI accounts for as much as a third of spinal cord injuries but few animal studies of this injury have been conducted and no effective therapies are available to reverse flaccid paralysis.

In rats, the lumbosacral (L1-S5) spinal cord is located in within the T11-L1 vertebra. Unlike humans who have 12 thoracic vertebrae, rats (and other sub-human animals) have 13 thoracic vertebrae. Like humans, the rat cauda equina occupies the spinal canal below L1. The rostral lumbar cord contains the CPG and injuries of the L1-L2 spinal cord causes severe disruptions of locomotion. While injuries of the L3-L5 spinal cord do not prevent locomotion, they cause flaccid paralysis of the muscles that control the foot, as well as the pelvic organs.

We therefore sought to develop a lumbosacral rat contusion model of SCI that would mimic the human condition. First, we back-labeled the tibialis and common peroneal branches of the

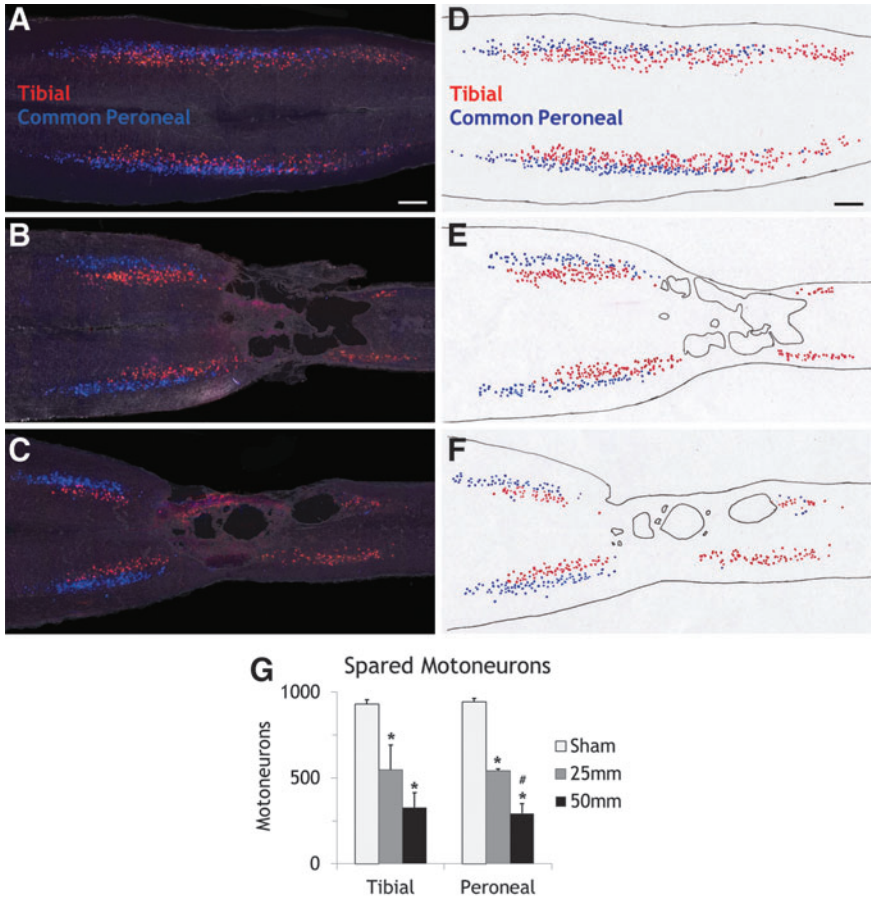

FIG. 5. Retrograde labeling of spared motoneurons. **(A–C)** are exemplary images of contused spinal cords at T13/L1 from the Sham, 25 mm and 50 mm injury groups, respectively. **(D–F)** are camera lucida drawings corresponding to A-C, indicating counted motoneurons. Scale bar (A-F), 500 μm. **(G)** shows a graph of the number of counted spared motoneurons back-labeled from the tibial and peroneal nerves in the Sham ($n=4$), 25 mm ($n=4$), and 50 mm ($n=4$) injury groups. The error bars (D) indicate standard deviation. * indicates $p<0.05$ versus the Sham group, # indicates $p<0.05$ versus the 25 mm group.

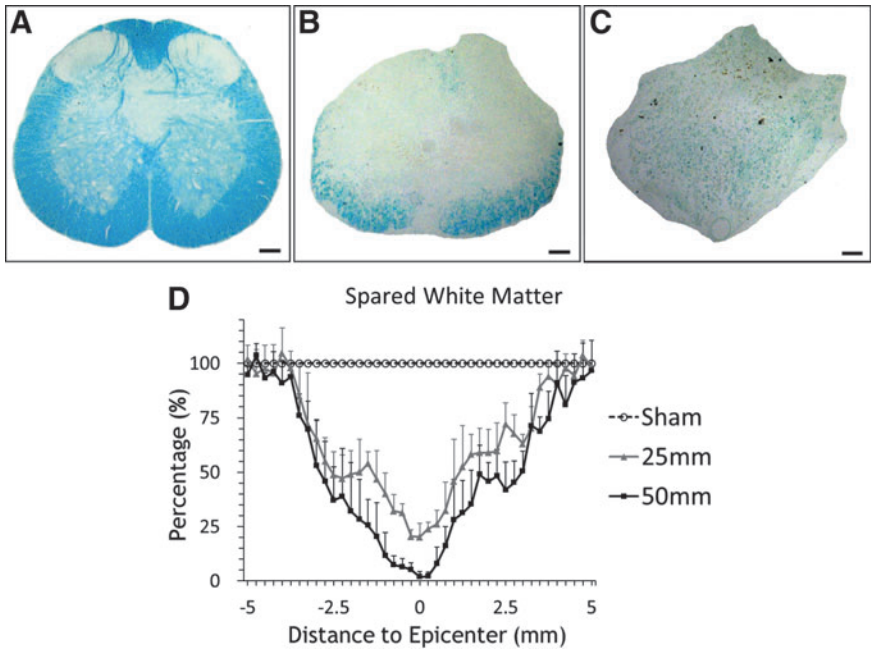

FIG. 6. Fast blue staining of white matter. **(A)** Cross-section in Group Sham. **(B)** Epicenter of Group 25 mm. **(C)** Epicenter of Group 50 mm. **(D)** Percentage of spared white matter compared with Group Sham. Animal numbers are the same as in Figure 4. Scale bar (A–C), 200 μm. The error bars (D) indicate standard deviation.

sciatic nerve with fluorescent dyes and found that back-labeled tibial and peroneal motoneurons are located at L3-L5 spinal cord. The L4 spinal cord is located at the T13/L1 vertebral junction. We chose to contuse the spinal cord at this level. Second, we contused the spinal cord by dropping a 10-g weight 25 or 50 mm onto the L4 spinal cord. This injury caused consistent changes in both walking and static footprints of the rats.

Histological analyses of the spinal cord, peripheral nerves, and muscles showed remarkably consistent losses of motoneurons and white matter, as well as substantial changes in axon diameter, myelin thickness of peroneal and tibial nerves, and cross-sectional areas of the gastrocnemius and anterior tibialis muscles. Surprisingly, we did not find a change in the number of axons in the peripheral nerves after 25 and 50 mm weight drop contusions. These findings will be discussed in sequence below.

The contusion site

We chose to contuse the L4-L5 spinal cord at the junction of T13/L1 vertebra for various reasons. This is a readily identifiable site that contains the motoneuronal columns of the peroneal and tibialis nerves. In addition to damaging motoneurons, the contusion also damages descending and ascending spinal tracts to the sacral segments that control the pelvic organs. Also, it does not damage the upper lumbar segments that contain the locomotor CPG, which would severely disrupt locomotor function.

Magnuson and colleagues[36] had earlier reported the effects of contusing rat L3-L4 spinal cord at vertebral level T13, causing mild locomotor deficits and relatively little change of the Basso-Beattie-Bresnahan (BBB) locomotor scores. Thoracic spinal cord contusions interrupt ascending and descending pathways[18,25,37] to and from the lumbosacral cord, causing severe deficits of hindlimb locomotion. The BBB locomotor score was designed to reflect the loss and sequence of locomotor recovery after thoracic SCI.

In contrast, contusions of L1-L2 spinal cord cause severe locomotor deficits due to damage of the CPG located at L1-L2.[42,43] Magnuson and colleagues[17] confirmed this by injecting kainic acid (KA), an excitotoxin that selectively damages gray matter and spares white matter. KA injected into thoracic cord (T10) did not affect walking. However, injection of KA into the L1-L2 cord caused severe locomotor deficits. The CPG contains the neuronal circuitry required to generate functional locomotor patterns[44,45] and plays a crucial role in restoring hindlimb locomotion after SCI.[46,47] We contused the L4-L5 cord to avoid compromising the CPG.[48]

The result is a rat with lumbosacral SCI that can walk but has weakness of plantar flexion and toe spread, both of which can be easily documented by analyzing walking and standing footprints. Motoneuronal loss can be readily quantified by back-filling the tibial and deep peroneal nerves with fluorescent dyes, as well as by changes in peripheral nerve and muscle fiber analysis. The injury can be varied to cause partial or complete loss of white matter by increasing the height of the weight drop from 25 mm to 50 mm.

Motoneuronal loss

As shown by retrograde labeling after injury (Fig. 5), the motoneuron columns of the common peroneal and tibial nerves extend above and below the injury site. The overall length of the common peroneal and tibial motoneuron pools were 4.71 mm and 5.01 mm respectively, consistent with previous studies showing motoneuron pools in the adult rat extending 3–5 mm and spanning more than one spinal segment.[49] As shown in NeuN stained cross-sections (Fig. 4), large, darkly stained motoneurons in the ventral horns were absent in 1.50 mm and 3.75 mm longitudinal gaps in the 25 mm and 50 mm groups.

Peroneal motoneurons are more lateral and rostral than tibial motoneurons, consistent with previous reports.[50,51] The L1 spinal cord is located at the T12 vertebra, the L2 spinal cord at the rostral end of T13 vertebra, the L3 and L4 spinal cord at the caudal end of T13 vertebra and the disc of T13/L1.[36] Kaizawa and Takahashi[50,52] described sciatic motoneurons at mid L4 through L6 spinal segments. Peroneal motoneurons are located at L3-L4 and rostral L5; tibial motor neurons are located in L4, L5, and the rostral L6 spinal cord.[49,51]

The 50-mm L4-5 weight drop contusion expectedly caused greater motoneuronal and white matter loss than the 25-mm weight drop but still without significant locomotor deficit. Previously, Magnuson and colleagues[36] found that a L3-4 contusion equivalent to 25 mm weight drop caused motoneuron loss restricted to a 2 mm length of cord, not enough to induce severe locomotor deficits. Schrimsher and Reier[53] likewise showed that motoneuron loss confined to the C4/5 spinal segments did not induce severe forelimb functional deficits.

This lumbosacral SCI model, therefore, is suitable for assessing motoneuronal replacement therapies. The motoneurons can be readily identified and counted. Successful regeneration of motoneuronal axons into the ventral roots and out the peripheral nerves can be documented by back-labeling axons from the peroneal and tibial nerves. Successful reinnervation of the motoneurons can be readily assessed histologically. The consequences of the motoneuronal loss or replacement can be readily quantified from footprint analyses.

Footprint analyses

The BBB test reflects recovery of multi-joint hindlimb locomotor function after thoracic SCI.[54,55] BBB scores recover rapidly after L4-L5 contusion because the model preserves femoral motoneurons and the CPG. Although the rats are able to walk and usually recover BBB scores of greater than 15, their walking is not normal and the effects of the contusion can be determined readily from footprint analysis.

Rats normally stand on their toes and their hind footprints normally show all five toes and footpads at the base of the toes. The toes should be spread and their heels should not touch the ground. Coming from the L4, L5, L6, S1, and S2 spinal roots, the common peroneal nerve innervates the short head of the biceps femoris and peroneus muscles that contribute to knee and plantar flexion of the feet (ankle extension). Injury to peroneal motoneurons weaken plantar flexion so that the rat rests more of its feet, including its heels, on the ground and hence produces a longer footprint (Fig. 2) when walking.

The tibial nerve comes from similar spinal roots (L4, L5, S1, S2, and S3) to innervate the gastrocnemius, popliteus, soleus, and plantaris muscles that also contribute to plantar flexion. In the foot, the tibial nerve divides into medial and lateral plantaris branches. The former supplies the abductor hallucis, flexor digitorum brevis, flexor hallucis brevis, and the first lumbrical muscles, which control the lateral foot and toe movements. The latter supplies the quadratus plantae, flexor digiti minimi, adductor hallucis, the interossei, and the second to fourth lumbricals. Damage to tibial motoneurons paralyzes the feet and prevent spreading of the toes during standing and walking.

Thus, changes in footprint length and toe spread reflect damage to the peroneal and tibial motoneurons. From two to six weeks after injury, footprint lengths, toe spreading and intermediate toe

spreading in the 25 mm and 50 mm groups differed significantly from those of the Sham group, as well as each other. The SFI in particular showed large and consistent changes. This should be a very sensitive measure of both neuroprotection, as well as restoration of function.

Walking versus standing footprints

We used both the SFI and SSI to assess foot function. Introduced in early 1980s[56] and later modified by Bain and colleagues[57] SFI was widely used to assess functional recovery of the sciatic nerve in rats.[40,58–62] The SFI is not usually used to assess foot recovery after SCI because the rats must walk to produce interpretable footprints.[63] SSI is technically easier to do than footprint analysis of walking, has all advantages of walking footprints, and produces results that correlate highly with dynamic footprint analysis.[41]

Foot print length during walking has been used alone as a behavioral test in a tibial nerve crush and transection model.[64] Toe spreading also has been used to evaluate behavioral changes in a lumbar (L4-6) dorsal root ganglion injury model in rats,[65] thoracic rat SCI,[63] a rat Achilles tendon rupture model[66] and a sciatic nerve injury model.[67] Static toe spread correlates with toe spread in walking foot prints and has turned out to be a useful parameter for measuring functional recovery after sciatic nerve injury.[41]

Both SFI and SSI turned out to be reliable behavioral tests for L4-L5 lumbar SCI. Both indices fell precipitously after injury in the 25 mm and 50 mm groups then recovered partially, while both indices remained stable in Sham rats (Fig. 2 and Fig. 3). ANOVA indicated that SFI and SSI differed significantly in the three treatment groups. SFI and SSI in Group 25 mm were always higher than Group 50 mm at all times observed after surgery. Our results suggested that both SFI and SSI are reliable behavioral tests to assess rats with L4-L5 SCI.

Walking footprints cannot be collected if the animal cannot walk. Individual and motivational factors also can affect walking velocity and SFI.[68,69] To reduce such variability, we pre-trained the rats for walking track analysis, measured five pairs of footprints from each rat before and after surgery, and acquired only footprints from the middle of the walking track and when walking pace was stable. Static toe footprints are easier to collect, does not require walking animals, and correlate with injury severity.[41] However, walking footprints are more sensitive and have smaller standard errors of means.

Gray matter damage

Contusions reproduce many manifestations of human SCI, including hemorrhagic necrosis, ischemia, and inflammation, central cavitation surrounded by gliosis and a spared rim of white matter.[13,70] Histological analysis of the spinal cord also revealed typical features of contusions seen in humans, including edema, inflammatory cell infiltration, and cystic cavity formation.[53] Dropping a weight onto the L4-L5 spinal cord damaged both gray and white matter at the injury site.

Gray matter damage is apparent from coronal sections of the contusion site. At the epicenter, no motoneurons were left at the injury site ± 2 mm of a 50 mm impact epicenter. In fact, no neurons of any kind were present at the impact epicenter (Fig. 4), although both motoneurons and other neurons were present at ± 2.5 mm from the injury epicenter. Note the greater destruction of dorsal spinal cord and the enlarged ventral spinal artery in the ventral sulcus. This pattern differs from contused thoracic spinal cords, which tend to have equally distributed circumferential damage and less ventral spinal artery dilation.[71]

Spinal cords injured with 25 mm weight drops had more spared motoneurons than rats injured with 50 mm weight drops. Retrograde labeling of peroneal and tibial neurons with Fluoro-Ruby and Fluoro-Gold allowed comparison of two populations of spared motoneurons (Fig. 5). Surprisingly, of about 950 backfilled motoneurons counted from each nerve, 25 mm and 50 mm contusions reduced the number of tibial and peroneal motoneurons almost identically by about 43% and 73%, respectively.

Earlier studies by Magnuson and colleagues[17] reported that injection of the neurotoxin kainic acid in the T9 spinal cord killed gray matter and preserved white matter with little effect on locomotor deficits in rats. However, the same injections into L2 spinal cord caused only gray matter damage with no white matter loss, but the rats showed severe locomotor deficits. Likewise, L2 contusions cause severe locomotor deficits. The locomotor central pattern generator is located at L2. The L4-5 contusion should have spared the central pattern generator but damaged its connections to peroneal and tibial motoneurons that control the ankles and feet, as well as the peroneal and tibial motoneurons themselves.

We chose to do the contusion at L4-5 to avoid damaging the L2 central pattern generator. Damage to the central pattern generator would disrupt walking even if the lower hindlimb motoneurons were intact. The L4-5 contusion model preserved the central pattern generator so that the rats could still walk, allowing investigators to assess effects of neuronal replacement therapy on the muscles controlling the ankle and foot. Of course, an L2 contusion would be useful for assessing therapies aimed at replacing the proximal limb motoneurons and rebuilding the central pattern generator, both daunting tasks.

White matter damage

The contusion also clearly damaged white matter. Spinal cords in the 50 mm group had significantly less spared white matter than the 25 mm group. As shown in Figure 6, the 25 mm group had 20% spared white matter at the epicenter, compared with nearly 0% in the 50 mm group. More white matter was spared on the ventral side than the dorsal side. In thoracic spinal cord injuries, white matter sparing correlates with locomotor scores.[72] However, in lumbosacral injuries, white matter sparing and injury severity do not predict BBB scores, although the footprint indices corresponded to injury severity and motoneuronal loss.

FIG. 7. Measurements of myelinated axons after surgery. **(A–C)** shows exemplary images of combined silver and fast blue staining of tibial nerve in the Sham, 25 mm, and 50 mm injury groups, respectively. Axons were stained black and surrounding myelin sheathes were stained blue. **(D)** shows the numbers of myelinated axon in tibial and peroneal nerves of the three injury groups. **(E–G)** are higher magnification images of tibial nerve in the Sham, 25 mm, and 50 mm, groups, respectively. Arrows indicate densely silver-stained axon bulbs. **(H)** shows mean axon diameters in the three injury groups. **(I)** shows myelin sheath thickness in the three injury groups. Scale bar (A–C), 100 μm; (E–G), 10 μm. The error bars (D, H, I) indicate standard deviation. * indicates $p < 0.05$ versus Sham; # indicates $p < 0.05$ versus 25 mm. The data represent means and standard errors of means from 3 rats from the Sham group and 4 rats each from the 25 mm and 50 mm groups.

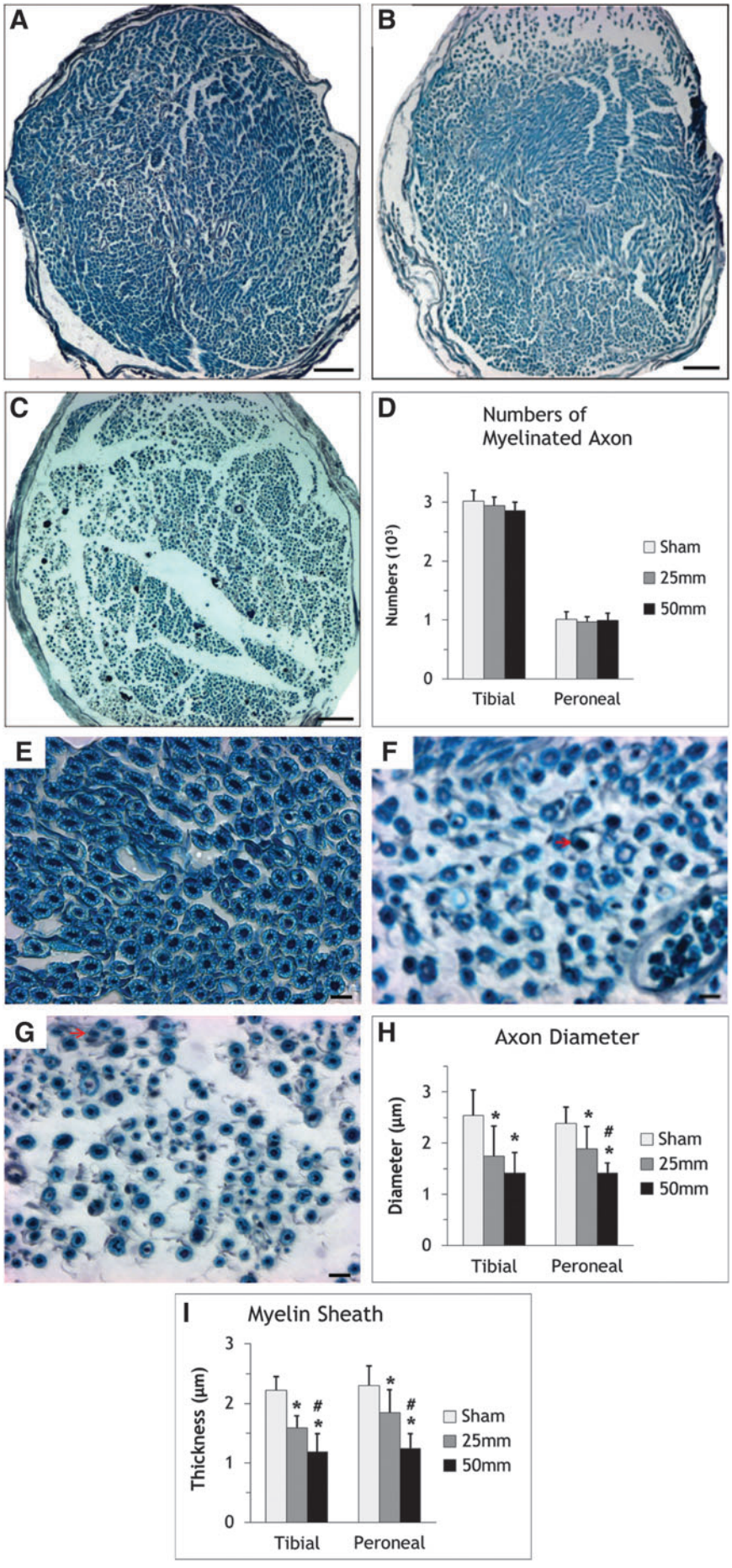
A
B
C
D
Numbers of
Myelinated Axon
Numbers (10^3)
3
2
1
0
Tibial
Peroneal
Sham
25mm
50mm
E
F
G
H
Axon Diameter
Diameter (μm)
*
#
I
Myelin Sheath
Thickness (μm)

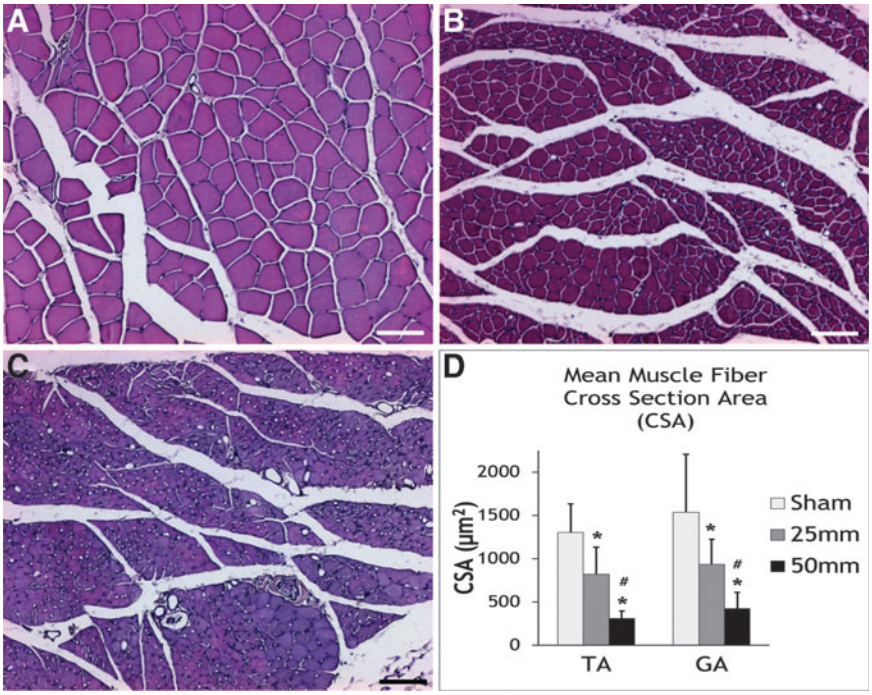

FIG. 8. Histologic changes of muscles. **(A–C)** show exemplary images of hematoxylin and eosin (H & E) stained gastrocnemius (GA) muscles in the Sham (A), 25 mm (B), and 50 mm (C) groups at six weeks after surgery. Scale bar (A–C), 100 μm. **(D)** Mean muscle fiber cross-sectional areas (CSA) of tibialis anterior (TA) and GA muscle in the Sham (n = 3), 25 mm ($n = 4$), and 50 mm ($n = 4$) groups. The error bars indicate standard deviation. Mean muscle fiber CSA in the 25 mm and 50 mm groups were significantly smaller than in the Sham group and from each other. * indicates $p < 0.05$ versus the Sham group; # indicates $p < 0.05$ versus 25 mm group.

Note the presence of blue-stained myelinated axons in the central part of the spinal cord contused with the 50 mm weight drop. These faint blue stains were not included in the spared white matter analysis. Earlier studies described this phenomenon in contused thoracic spinal cords (i.e., many axons are growing in the central part of the spinal cord), particularly in severely contused spinal cords and that these axons are myelinated by six weeks after injury.[71,73] Normally, no axons are present in the central part of the spinal cord. Spontaneous axonal growth appears to be occurring at contusion site of lumbosacral model, like the thoracic spinal cord contusion model.

The loss of white matter at L4-5 indicates disruption of ascending and descending connections between the proximal cord and supraspinal centers. The rats should have loss of sensation from L4-5 and sacral segments, as well as supraspinal control of the foot and sacral functions. We did not investigate the sacral nuclei in this study but suspect that the proximal sacral nuclei probably damaged by the L4-5 contusion and hence caused the difficulty we had with bladder care of the rats. However, the observation that the rats continue to defecate suggests that the lower sacral nuclei may have been preserved.

Peripheral nerve axon counts

The L4-L5 injury eliminated many motoneurons. Based on the counts of backfilled neurons (Fig. 5), the 25-mm weight drop eliminated about 40% of both tibial and peroneal motoneurons, while the 50 mm weight drop eliminated about 70% of both tibial and peroneal motoneurons. ANOVA indicated significant differences in spared tibial ($p = 0.001$) and peroneal motoneurons ($p < 0.0001$) among the three injury groups. For the tibial nerve, post hoc tests indicated significant differences between the Sham and 25 mm groups ($p = 0.0126$) and the Sham and 50 mm groups ($p = 0.001$) but no difference between the 25 mm and 50 mm groups ($p = 0.0971$). For the peroneal nerve, post hoc tests indicated significant differences between the Sham and 25 mm groups ($p = 0.0003$), the Sham and 50 mm groups ($p < 0.0001$), and the 25 mm and 50 mm groups ($p = 0.0031$).

We therefore expected to see significant loss of axons in the peripheral nerves. Combined silver and LFB staining clearly showed axons and their myelin sheaths. However, we found no significant difference of myelinated axon counts among the Sham, 25 mm, and 50 mm groups (Fig. 7D), even though there were significant differences of motoneuron loss among these groups. One explanation is that the motor axons are degenerating slowly (i.e., like Wallerian degeneration of central axons). The light microscopic findings should be confirmed with ultrastructural, tracing, and neurophysiological studies at earlier and later times.

Rapid degeneration of peripheral axons after peripheral nerve injury is well known.[74–76] However, little has been reported concerning speed of peripheral nerve degeneration after SCI.[77,78] Delayed Wallerian degeneration occurs in peripheral nerves in alcoholic neuropathy,[74] triethyl- and trimethyl-tin lesions,[79] Werdnig-Hoffmann disease,[80] and other conditions.[81] It would be of interest to see if lumbosacral SCI triggers the Wld(s) gene that slows down Wallerian degeneration[82,83] and other genes that may regulate Wallerian degeneration.[84,85]

Axon diameters, myelin sheath thickness, and muscle changes

Although lumbosacral contusion did not significantly reduce axon counts in peroneal and tibial nerves compared to Sham-injured rats, we observed striking reductions in axon diameters and

myelin sheath thickness in the peroneal and tibial nerves after L4-L5 SCI, as well as muscle atrophy similar to those observed in diaphragm after phrenic motoneuronal loss.[19] The changes of axon thickness and myelin are similar to a previous study that found reduced diameter and myelin sheath thickness of optic axons after encephalomyelitis.[86] ANOVA indicated that rats in the 50 mm group had significantly thinner axon diameter and myelin sheath in the peroneal, but not tibial, nerve of rats in the 25 mm group ($p < 0.05$), and both the 25 mm and 50 mm groups had thinner axons and myelin than the Sham group ($p < 0.05$) in both nerves.

These observations suggest that many axons of motoneurons damaged by the contusion may not have degenerated but have undergone atrophy at six weeks. Occasionally, we saw densely silver-stained and enlarged axons (red arrow, Fig. 7F) without surrounding myelin. These may be retracted axon bulbs. Thus, while axon counts in the tibial and common peroneal nerves do not reliably reflect motoneuron damage in the spinal cord, axon diameter and myelin sheath thickness do correspond to the severity of the spinal cord contusion and motoneuronal loss.

Muscular degeneration was clearly present at six weeks after injury. H&E staining showed both atrophied and degenerating myofibers in the TA and GA muscles. There may be other causes of the muscle atrophy besides motoneuronal loss, including non-use atrophy and contusion to spinal roots running alongside the L4-L5 lumbosacral spinal cord. Nevertheless, muscle fiber cross-sectional areas (CSA) were uniformly smaller in 50 mm-contused rats than in 25 mm–contused rats.

Drawbacks and opportunities

Our experiments revealed several drawbacks to the lumbosacral contusion model and the outcome measures that we chose. First, we had to study female rats because preliminary experiments suggested that male rats may have higher mortality rates due to development of flaccid paralysis and blood clots in the bladder (data unpublished). Female rats did not have this problem. The L4-L5 contusion may damage local circuitry for Onuf's nucleus, causing flaccid bladder paralysis.[87] Male rats have longer urethras and an external sphincter, making manual expression of the bladder more difficult. Female rats have a shorter urethra and only an internal bladder sphincter, which may make bladder expression easier. The model presents an interesting opportunity to test therapies to reverse bladder flaccidity in both male and female rats.

Second, we unexpectedly found that 25 mm and 50 mm contusions of the L4-L5 cord did not significantly change the number of myelinated axons in the peroneal or tibial nerves at six weeks although the nerves did show significant differences of axon diameters and myelin-sheath thickness. Waiting longer than six weeks after the injury may result in clearer patterns of axon loss. However, both GA and TA muscles showed severe atrophy that could be readily quantified from muscle fiber cross-sectional areas. These findings indicate that muscle changes are a more sensitive indicator of motoneuronal damage than peripheral nerve axon counts. On the other hand, our findings provide an opportunity to study slow axonal degeneration that occurs after lumbosacral contusion, very different from rapid axonal degeneration after peripheral nerve injury.

Third, the two muscles (TA and GA) we studied did not correspond directly to the two nerves (tibial and deep peroneal) that we backfilled. In retrospect, we probably should have assessed the long peroneus and the abductor hallucis muscles, which, respectively, would have better reflected the common peroneal and tibial nerve branches that we backfilled. On the other hand, our data shows that L4-5 contusions cause significant atrophy of the TA and GA, two major muscles innervated by the tibial nerve. It would be of interest to do electrophysiology tests to confirm denervation despite persistence of the axons.

Choice of outcome measures

The BBB score is a popular approach to assessing hindlimb function in rats after spinal cord injury.[54,88] We chose not to apply BBB to this model because rats with lumbosacral injuries do not exhibit many of the behavioral changes that BBB score use to assess hindlimb function. BBB scores depend on graded recovery of hip/knee/ankle joint movements, weight support, forelimb/hindlimb coordination, foot eversion on contact and liftoff, toe clearance, tail position, and postural stability. Rats with lumbosacral injures have intact motor control of hip and knee joints and therefore can support their weight and walk with forelimb/hindlimb coordination. However, lumbosacral injuries paralyze the plantar and foot muscles, so that the rats no longer walk on their toes but shuffle along with their heels on the ground. Their feet clench in flexion and they cannot spread their toes. The tail touches the ground. Both the 25 mm and 50 mm rats will have a BBB score of 15 and stay at that level.

Two other commonly-used measures of hindlimb were not useful for distinguishing lumbosacral injury severity in the rats. For example, due to their plantar weakness and inability to spread the toes, rats with lumbosacral injuries cannot support their weight on rungs of ladders and therefore perform poorly on the horizontal ladder test. Likewise, the rats cannot gain traction on inclined surfaces and tend to slide off even moderately inclined planes. Treatments that restore foot innervation may allow the rats to improve on these two tests but these tests are not useful for distinguishing between 25 mm and 50 mm contusions.

Finally, although our original intent was to study the bladder, bowel, and sexual function as well as walking in this model, we encountered significant difficulties caring for male rats with flaccid bladders resulting from lumbosacral injuries. In female rats, urinary retention with overflow incontinence occurs at an early stage after L4-5 contusion. With spinal cord recovery and the appearance of detrusor hyperreflexia, urge urinary incontinence appears. The rats defecated without difficulty. We therefore chose to wait until we figure we can determine how to care for lumbosacral injured male rats before doing this study.

Conclusion

Traditional spinal cord injury models have focused on mostly the thoracic and cervical spinal cord, ignoring the lumbosacral spinal cord injury, which is much more common than usually thought. As much as a third of spinal cord traumas may involve the lumbosacral spinal cord. Because the lumbar enlargement and sacral nuclei are present in the lumbosacral cord, injuries to that region of the spinal cord result in flaccid paralysis of lower hindlimb muscles and pelvic organs, including the bladder and anal sphincters. Restoring function to lumbosacral spinal cord injury will require more than regeneration of long spinal tracts. Motoneuronal replacement will be necessary. Unfortunately, no standardized model of lumbosacral spinal cord contusion is available for testing such therapies.

We therefore developed a lumbosacral spinal cord contusion to address this gap. Our experiments show that motoneurons backfilled from the deep peroneal and the tibial nerves reside in the L4-L5 spinal cord located at the T13/L1 vertebral junction. Contusion

of the spinal cord at the T13/L1 vertebral junction produces graded loss of 40% to 70% of motoneurons that contribute axons to both nerve, reflected in significant and readily quantified changes in walking footprint lengths and standing toe spread. The contusions also produce significant reductions of axon diameter and myelin sheath thickness in the deep peroneal and tibial nerves, as well as severe and reproducible graded atrophy of the gastrocnemius and tibialis anterior muscles.

This model closely mimics human lumbosacral injuries, including the flaccid paralysis of lower limb muscles and development of flaccid bladder paralysis. The model should allow the study and testing of therapies aimed at preventing and restoring function in lumbosacral spinal cord contusions. Both the injury model and the outcome measures should be readily implemented in most laboratories that do spinal cord injury studies. This model utilizes simple and reliable outcome measures that do not require costly instrumentation and specialized facilities.

Acknowledgments

We thank Bor Tom Ng, Hock Ng, and Sean O'Leary for their invaluable assistance and technical help in all the procedures and animal care. We are grateful to the donors of the Spinal Cord Injury Project, and particularly Mr. Dennis Chan for his generous support of lumbosacral spinal cord injury studies, at the W. M. Keck Center for Collaborative Neuroscience at Rutgers University. Dr. Junxiang Wen was generously supported by a fellowship under the State Scholarship Fund by the China Scholarshop Council.

Author Disclosure Statement

No competing financial interests exist.

References

1. National Spinal Cord Injury Statistical Center. (2013). Spinal cord injury facts and figures at a glance. J. Spinal Cord Med. 36, 1–2.
2. Beric, A., Dimitrijevic, M.R., and Light, J.K. (1987). A clinical syndrome of rostral and caudal spinal injury: neurological, neurophysiological and urodynamic evidence for occult sacral lesion. J. Neurol. Neurosurg. Psychiatry 50, 600–606.
3. Maynard, F.M., Karunas, R.S., and Waring, W.P., 3rd (1990). Epidemiology of spasticity following traumatic spinal cord injury. Arch. Phys. Med. Rehabil. 71, 566–569.
4. Wang, H.F., Yin, Z.S., Chen, Y., Duan, Z.H., Hou, S., and He, J. (2013). Epidemiological features of traumatic spinal cord injury in Anhui Province, China. Spinal Cord 51, 20–22.
5. Doherty, J.G., Burns, A.S., O'Ferrall, D.M., and Ditunno, J.F., Jr. (2002). Prevalence of upper motor neuron vs lower motor neuron lesions in complete lower thoracic and lumbar spinal cord injuries. J. Spinal Cord Med. 25, 289–292.
6. Khaing, Z.Z., Geissler, S.A., Jiang, S., Milman, B.D., Aguilar, S.V., Schmidt, C.E., and Schallert, T. (2012). Assessing forelimb function after unilateral cervical spinal cord injury: novel forelimb tasks predict lesion severity and recovery. J. Neurotrauma 29, 488–498.
7. Rooney, G.E., Endo, T., Ameenuddin, S., Chen, B., Vaishya, S., Gross, L., Schiefer, T.K., Currier, B.L., Spinner, R.J., Yaszemski, M.J., and Windebank, A.J. (2009). Importance of the vasculature in cyst formation after spinal cord injury. J. Neurosurg. Spine 11, 432–437.
8. Ren, L.Q., Wienecke, J., Chen, M., Moller, M., Hultborn, H., and Zhang, M. (2013). The time course of serotonin 2C receptor expression after spinal transection of rats: an immunohistochemical study. Neuroscience 236, 31–46.
9. Cloud, B.A., Ball, B.G., Chen, B.K., Knight, A.M., Hakim, J.S., Ortiz, A.M., and Windebank, A.J. (2012). Hemisection spinal cord injury in rat: the value of intraoperative somatosensory evoked potential monitoring. J. Neurosci. Methods 211, 179–184.
10. Liu, K., Lu, Y., Lee, J.K., Samara, R., Willenberg, R., Sears-Kraxberger, I., Tedeschi, A., Park, K.K., Jin, D., Cai, B., Xu, B., Connolly, L., Steward, O., Zheng, B., and He, Z. (2010). PTEN deletion enhances the regenerative ability of adult corticospinal neurons. Nat. Neurosci. 13, 1075–1081.
11. Dulin, J.N., Karoly, E.D., Wang, Y., Strobel, H.W., and Grill, R.J. (2013). Licofelone modulates neuroinflammation and attenuates mechanical hypersensitivity in the chronic phase of spinal cord injury. J. Neurosci. 33, 652–664.
12. Ward, P.J. and Hubscher, C.H. (2012). Persistent polyuria in a rat spinal contusion model. J. Neurotrauma 29, 2490–2498.
13. Choo, A.M., Liu, J., Liu, Z., Dvorak, M., Tetzlaff, W., and Oxland, T.R. (2009). Modeling spinal cord contusion, dislocation, and distraction: characterization of vertebral clamps, injury severities, and node of Ranvier deformations. J. Neurosci. Methods 181, 6–17.
14. Young, W. (2002). Spinal cord contusion models. Prog. Brain Res. 137, 231–255.
15. Ahn, M., Lee, C., Jung, K., Kim, H., Moon, C., Sim, K.B., and Shin, T. (2012). Immunohistochemical study of arginase-1 in the spinal cords of rats with clip compression injury. Brain Res. 1445, 11–19.
16. Weaver, L.C., Dekaban, G.A., and Brown, A. (2012). Anti-CD11d monoclonal antibody treatment for rat spinal cord compression injury. Exp. Neurol. 233, 612–614.
17. Magnuson, D.S., Trinder, T.C., Zhang, Y.P., Burke, D., Morassutti, D.J., and Shields, C.B. (1999). Comparing deficits following excitotoxic and contusion injuries in the thoracic and lumbar spinal cord of the adult rat. Exp. Neurol. 156, 191–204.
18. Behrmann, D.L., Bresnahan, J.C., and Beattie, M.S. (1994). Modeling of acute spinal cord injury in the rat: neuroprotection and enhanced recovery with methylprednisolone, U-74006F and YM-14673. Exp. Neurol. 126, 61–75.
19. Nicaise, C., Hala, T.J., Frank, D.M., Parker, J.L., Authelet, M., Leroy, K., Brion, J.P., Wright, M.C., and Lepore, A.C. (2012). Phrenic motor neuron degeneration compromises phrenic axonal circuitry and diaphragm activity in a unilateral cervical contusion model of spinal cord injury. Exp. Neurol. 235, 539–552.
20. Dunham, K.A., Siriphorn, A., Chompoopong, S., and Floyd, C.L. (2010). Characterization of a graded cervical hemicontusion spinal cord injury model in adult male rats. J. Neurotrauma 27, 2091–2106.
21. Aguilar, R.M. and Steward, O. (2010). A bilateral cervical contusion injury model in mice: assessment of gripping strength as a measure of forelimb motor function. Exp. Neurol. 221, 38–53.
22. Anderson, K.D., Sharp, K.G., and Steward, O. (2009). Bilateral cervical contusion spinal cord injury in rats. Exp. Neurol. 220, 9–22.
23. Gensel, J.C., Tovar, C.A., Hamers, F.P., Deibert, R.J., Beattie, M.S., and Bresnahan, J.C. (2006). Behavioral and histological characterization of unilateral cervical spinal cord contusion injury in rats. J. Neurotrauma 23, 36–54.
24. Anderson, K.D., Sharp, K.G., Hofstadter, M., Irvine, K.A., Murray, M., and Steward, O. (2009). Forelimb locomotor assessment scale (FLAS): novel assessment of forelimb dysfunction after cervical spinal cord injury. Exp. Neurol. 220, 23–33.
25. Saruhashi, Y., Young, W., and Perkins, R. (1996). The recovery of 5-HT immunoreactivity in lumbosacral spinal cord and locomotor function after thoracic hemisection. Exp. Neurol. 139, 203–213.
26. Weishaupt, N., Vavrek, R., and Fouad, K. (2013). Training following unilateral cervical spinal cord injury in rats affects the contralesional forelimb. Neurosci. Lett. 539, 77–81.
27. Streijger, F., Beernink, T.M., Lee, J.H., Bhatnagar, T., Park, S., Kwon, B.K., and Tetzlaff, W. (2013). Characterization of a cervical spinal cord hemicontusion injury in mice using the infinite horizon impactor. J. Neurotrauma 30, 869–883.
28. Sandrow, H.R., Shumsky, J.S., Amin, A., and Houle, J.D. (2008). Aspiration of a cervical spinal contusion injury in preparation for delayed peripheral nerve grafting does not impair forelimb behavior or axon regeneration. Exp. Neurol. 210, 489–500.
29. Onifer, S.M., Nunn, C.D., Decker, J.A., Payne, B.N., Wagoner, M.R., Puckett, A.H., Massey, J.M., Armstrong, J., Kaddumi, E.G., Fentress, K.G., Wells, M.J., West, R.M., Calloway, C.C., Schnell, J.T., Whitaker, C.M., Burke, D.A., and Hubscher, C.H. (2007). Loss and spontaneous recovery of forelimb evoked potentials in both the adult rat cuneate nucleus and somatosensory cortex following contusive cervical spinal cord injury. Exp. Neurol. 207, 238–247.
30. Marchand, F., Tsantoulas, C., Singh, D., Grist, J., Clark, A.K., Bradbury, E.J., and McMahon, S.B. (2009). Effects of Etanercept and Minocycline in a rat model of spinal cord injury. Eur. J. Pain 13, 673–681.

31. Bennett, A.D., Everhart, A.W., and Hulsebosch, C.E. (2000). Intrathecal administration of an NMDA or a non-NMDA receptor antagonist reduces mechanical but not thermal allodynia in a rodent model of chronic central pain after spinal cord injury. Brain Res. 859, 72–82.
32. Barritt, A.W., Davies, M., Marchand, F., Hartley, R., Grist, J., Yip, P., McMahon, S.B., and Bradbury, E.J. (2006). Chondroitinase ABC promotes sprouting of intact and injured spinal systems after spinal cord injury. J. Neurosci. 26, 10856–10867.
33. Faulkner, J.R., Herrmann, J.E., Woo, M.J., Tansey, K.E., Doan, N.B., and Sofroniew, M.V. (2004). Reactive astrocytes protect tissue and preserve function after spinal cord injury. J. Neurosci. 24, 2143–2155.
34. Fukuda, S., Nakamura, T., Kishigami, Y., Endo, K., Azuma, T., Fujikawa, T., Tsutsumi, S., and Shimizu, Y. (2005). New canine spinal cord injury model free from laminectomy. Brain Res. Brain Res. Protoc. 14, 171–180.
35. Shunmugavel, A., Martin, M.M., Khan, M., Copay, A.G., Subach, B.R., Schuler, T.C., and Singh, I. (2013). Simvastatin ameliorates cauda equina compression injury in a rat model of lumbar spinal stenosis. J. Neuroimmune Pharmacol. 8, 274–286.
36. Magnuson, D.S., Lovett, R., Coffee, C., Gray, R., Han, Y., Zhang, Y.P., and Burke, D.A. (2005). Functional consequences of lumbar spinal cord contusion injuries in the adult rat. J. Neurotrauma 22, 529–543.
37. Basso, D.M., Beattie, M.S., and Bresnahan, J.C. (1996). Graded histological and locomotor outcomes after spinal cord contusion using the NYU weight-drop device versus transection. Exp. Neurol. 139, 244–256.
38. Bain, J.R., Mackinnon, S.E., Hudson, A.R., Falk, R.E., Falk, J.A., Hunter, D.A., and Makino, A. (1989). Preliminary report of peripheral nerve allografting in primates immunosuppressed with cyclosporin A. Transplant. Proc. 21, 3176–3177.
39. Dijkstra, J.R., Meek, M.F., Robinson, P.H., and Gramsbergen, A. (2000). Methods to evaluate functional nerve recovery in adult rats: walking track analysis, video analysis and the withdrawal reflex. J. Neurosci. Methods 96, 89–96.
40. Luis, A.L., Amado, S., Geuna, S., Rodrigues, J.M., Simoes, M.J., Santos, J.D., Fregnan, F., Raimondo, S., Veloso, A.P., Ferreira, A.J., Armada-da-Silva, P.A., Varejao, A.S., and Mauricio, A.C. (2007). Long-term functional and morphological assessment of a standardized rat sciatic nerve crush injury with a non-serrated clamp. J. Neurosci. Methods 163, 92–104.
41. Bervar, M. (2000). Video analysis of standing–an alternative footprint analysis to assess functional loss following injury to the rat sciatic nerve. J. Neurosci. Methods 102, 109–116.
42. Garcia-Alias, G., Valero-Cabre, A., Lopez-Vales, R., Fores, J., Verdu, E., and Navarro, X. (2006). Differential motor and electrophysiological outcome in rats with mid-thoracic or high lumbar incomplete spinal cord injuries. Brain Res. 1108, 195–204.
43. Cazalets, J.R., Borde, M., and Clarac, F. (1995). Localization and organization of the central pattern generator for hindlimb locomotion in newborn rat. J. Neurosci. 15, 4943–4951.
44. Rossignol, S., Chau, C., Brustein, E., Giroux, N., Bouyer, L., Barbeau, H., and Reader, T.A. (1998). Pharmacological activation and modulation of the central pattern generator for locomotion in the cat. Ann. N. Y. Acad. Sci. 860, 346–359.
45. Magnuson, D.S. and Trinder, T.C. (1997). Locomotor rhythm evoked by ventrolateral funiculus stimulation in the neonatal rat spinal cord in vitro. J. Neurophysiol. 77, 200–206.
46. Rossignol, S., Barriere, G., Alluin, O., and Frigon, A. (2009). Re-expression of locomotor function after partial spinal cord injury. Physiology (Bethesda) 24, 127–139.
47. Frigon, A. and Rossignol, S. (2006). Functional plasticity following spinal cord lesions. Prog. Brain Res. 157, 231–260.
48. Barriere, G., Leblond, H., Provencher, J., and Rossignol, S. (2008). Prominent role of the spinal central pattern generator in the recovery of locomotion after partial spinal cord injuries. J. Neurosci. 28, 3976–3987.
49. Nicolopoulos-Stournaras, S. and Iles, J.F. (1983). Motor neuron columns in the lumbar spinal cord of the rat. J. Comp. Neurol. 217, 75–85.
50. Kaizawa, J. and Takahashi, I. (1970). Motor cell columns in rat lumbar spinal cord. Tohoku J. Exp. Med. 101, 25–33.
51. Valero-Cabre, A., Tsironis, K., Skouras, E., Perego, G., Navarro, X., and Neiss, W.F. (2001). Superior muscle reinnervation after autologous nerve graft or poly-L-lactide-epsilon-caprolactone (PLC) tube implantation in comparison to silicone tube repair. J. Neurosci. Res. 63, 214–223.
52. Kaizawa, J. and Takahashi, I. (1970). Fiber analysis of the lumbar spinal roots and their sciatic branches in rats. Tohoku J. Exp. Med. 100, 61–74.
53. Schrimsher, G.W. and Reier, P.J. (1992). Forelimb motor performance following cervical spinal cord contusion injury in the rat. Exp. Neurol. 117, 287–298.
54. Basso, D.M., Beattie, M.S., and Bresnahan, J.C. (1995). A sensitive and reliable locomotor rating scale for open field testing in rats. J. Neurotrauma 12, 1–21.
55. Zorner, B., Filli, L., Starkey, M.L., Gonzenbach, R., Kasper, H., Rothlisberger, M., Bolliger, M., and Schwab, M.E. (2010). Profiling locomotor recovery: comprehensive quantification of impairments after CNS damage in rodents. Nat. Methods 7, 701–708.
56. de Medinaceli, L., Freed, W.J., and Wyatt, R.J. (1982). An index of the functional condition of rat sciatic nerve based on measurements made from walking tracks. Exp. Neurol. 77, 634–643.
57. Bain, J.R., Mackinnon, S.E., and Hunter, D.A. (1989). Functional evaluation of complete sciatic, peroneal, and posterior tibial nerve lesions in the rat. Plast. Reconstr. Surg. 83, 129–138.
58. Monte-Raso, V.V., Barbieri, C.H., Mazzer, N., Yamasita, A.C., and Barbieri, G. (2008). Is the Sciatic Functional Index always reliable and reproducible? J. Neurosci. Methods 170, 255–261.
59. Raso, V.V., Barbieri, C.H., Mazzer, N., and Fasan, V.S. (2005). Can therapeutic ultrasound influence the regeneration of peripheral nerves? J. Neurosci. Methods 142, 185–192.
60. Fernandes, M., Valente, S.G., Fernandes, M.J., Felix, E.P., Mazzacoratti Mda, G., Scerni, D.A., dos Santos, J.B., Leite, V.M., and Faloppa, F. (2008). Bone marrow cells are able to increase vessels number during repair of sciatic nerve lesion. J. Neurosci. Methods 170, 16–24.
61. Chung, C.L., Tsai, H.P., Lee, K.S., Chen, K.I., Wu, S.C., Kuo, Y.H., Winardi, W., Chen, I.C., and Kwan, A.L. (2012). Assisted peripheral nerve recovery by KMUP-1, an activator of large-conductance Ca(2+)-activated potassium channel, in a rat model of sciatic nerve crush injury. Acta Neurochir. (Wien) 154, 1773–1779.
62. Matsuda, K., Kakibuchi, M., Fukuda, K., Kubo, T., Madura, T., Kawai, K., Yano, K., and Hosokawa, K. (2005). End-to-side nerve grafts: experimental study in rats. J. Reconstr. Microsurg. 21, 581–591.
63. Behrmann, D.L., Bresnahan, J.C., Beattie, M.S., and Shah, B.R. (1992). Spinal cord injury produced by consistent mechanical displacement of the cord in rats: behavioral and histologic analysis. J. Neurotrauma 9, 197–217.
64. Yan, Y., Sun, H.H., Hunter, D.A., Mackinnon, S.E., and Johnson, P.J. (2012). Efficacy of short-term FK506 administration on accelerating nerve regeneration. Neurorehabil. Neural Repair 26, 570–580.
65. Liu, S., Brejot, T., Cressant, A., Bacci, J., Said, G., Tadie, M., and Heard, J.M. (2005). Reinnervation of hind limb extremity after lumbar dorsal root ganglion injury. Exp. Neurol. 196, 401–412.
66. Liang, J.I., Chen, M.Y., Hsieh, T.H., Liu, C.Y., Lam, C.F., Chen, J.J., and Yeh, M.L. (2012). Video-based gait analysis for functional evaluation of healing achilles tendon in rats. Ann. Biomed. Eng. 40, 2532–2540.
67. van Neerven, S.G., Bozkurt, A., O'Dey, D.M., Scheffel, J., Boecker, A.H., Stromps, J.P., Dunda, S., Brook, G.A., and Pallua, N. (2012). Retrograde tracing and toe spreading after experimental autologous nerve transplantation and crush injury of the sciatic nerve: a descriptive methodological study. J. Brachial Plex. Peripher. Nerve Inj. 7, 5.
68. Sedy, J., Urdzikova, L., Jendelova, P., and Sykova, E. (2008). Methods for behavioral testing of spinal cord injured rats. Neurosci. Biobehav. Rev. 32, 550–580.
69. Metz, G.A., Merkler, D., Dietz, V., Schwab, M.E., and Fouad, K. (2000). Efficient testing of motor function in spinal cord injured rats. Brain Res. 883, 165–177.
70. Bresnahan, J.C., Beattie, M.S., Stokes, B.T., and Conway, K.M. (1991). Three-dimensional computer-assisted analysis of graded contusion lesions in the spinal cord of the rat. J. Neurotrauma 8, 91–101.
71. Beattie, M.S., Bresnahan, J.C., Komon, J., Tovar, C.A., Van Meter, M., Anderson, D.K., Faden, A.I., Hsu, C.Y., Noble, L.J., Salzman, S., and Young, W. (1997). Endogenous repair after spinal cord contusion injuries in the rat. Exp. Neurol. 148, 453–463.
72. Schucht, P., Raineteau, O., Schwab, M.E., and Fouad, K. (2002). Anatomical correlates of locomotor recovery following dorsal and ventral lesions of the rat spinal cord. Exp. Neurol. 176, 143–153.

73. Hill, C.E., Beattie, M.S., and Bresnahan, J.C. (2001). Degeneration and sprouting of identified descending supraspinal axons after contusive spinal cord injury in the rat. Exp. Neurol. 171, 153–169.
74. Tredici, G. and Minazzi, M. (1975). Alcoholic neuropathy. An electron-microscopic study. J. Neurol. Sci. 25, 333–346.
75. Titelbaum, D.S., Frazier, J.L., Grossman, R.I., Joseph, P.M., Yu, L.T., Kassab, E.A., Hickey, W.F., LaRossa, D., and Brown, M.J. (1989). Wallerian degeneration and inflammation in rat peripheral nerve detected by in vivo MR imaging. AJNR Am. J. Neuroradiol. 10, 741–746.
76. George, R. and Griffin, J.W. (1994). Delayed macrophage responses and myelin clearance during Wallerian degeneration in the central nervous system: the dorsal radiculotomy model. Exp. Neurol. 129, 225–236.
77. Van De Meent, H., Hosman, A.J., Hendriks, J., Zwarts, M., Group, E.-S.S., and Schubert, M. (2010). Severe degeneration of peripheral motor axons after spinal cord injury: a European multicenter study in 345 patients. Neurorehabil. Neural. Repair 24, 657–665.
78. Ingebrigtsen, R. (1915). A Contribution to the Biology of Peripheral Nerves in Transplantation. J. Exp. Med. 22, 418–426.
79. O'Shaughnessy, D.J. and Losos, G.J. (1986). Peripheral and central nervous system lesions caused by triethyl- and trimethyltin salts in rats. Toxicol. Pathol. 14, 141–148.
80. Chien, Y.Y. and Nonaka, I. (1989). Peripheral nerve involvement in Werdnig-Hoffmann disease. Brain Dev. 11, 221–229.
81. Harper, P.A. and Healy, P.J. (1989). Neurological disease associated with degenerative axonopathy of neonatal Holstein-Friesian calves. Aust. Vet. J. 66, 143–144, 145–146.
82. Wang, M., Wu, Y., Culver, D.G., and Glass, J.D. (2001). The gene for slow Wallerian degeneration (Wld(s)) is also protective against vincristine neuropathy. Neurobiol. Dis. 8, 155–161.
83. Mi, W., Beirowski, B., Gillingwater, T.H., Adalbert, R., Wagner, D., Grumme, D., Osaka, H., Conforti, L., Arnhold, S., Addicks, K., Wada, K., Ribchester, R.R., and Coleman, M.P. (2005). The slow Wallerian degeneration gene, WldS, inhibits axonal spheroid pathology in gracile axonal dystrophy mice. Brain 128, 405–416.
84. Hughes, P.M., Wells, G.M., Perry, V.H., Brown, M.C., and Miller, K.M. (2002). Comparison of matrix metalloproteinase expression during Wallerian degeneration in the central and peripheral nervous systems. Neuroscience 113, 273–-287.
85. Krekoski, C.A., Neubauer, D., Graham, J.B., and Muir, D. (2002). Metalloproteinase-dependent predegeneration in vitro enhances axonal regeneration within acellular peripheral nerve grafts. J. Neurosci. 22, 10408–10415.
86. Guy, J., Ellis, E.A., Hope, G.M., and Emerson, S. (1991). Maintenance of myelinated fibre g ratio in acute experimental allergic encephalomyelitis. Brain 114 (Pt 1A), 281–294.
87. David, B.T. and Steward, O. (2010). Deficits in bladder function following spinal cord injury vary depending on the level of the injury. Exp. Neurol. 226, 128–135.
88. Basso, D.M., Beattie, M.S., Bresnahan, J.C., Anderson, D.K., Faden, A.I., Gruner, J.A., Holford, T.R., Hsu, C.Y., Noble, L.J., Nockels, R., Perot, P.L., Salzman, S.K., and Young, W. (1996). MASCIS evaluation of open field locomotor scores: effects of experience and teamwork on reliability. Multicenter Animal Spinal Cord Injury Study. J. Neurotrauma 13, 343–359.

Address correspondence to:
Wise Young, PhD, MD
W. M. Keck Center for Collaborative Neuroscience
D251 Nelson Biological Laboratory
604 Allison Road
Piscataway, NJ 08854-8082

E-mail: young@biology.rutgers.edu